University of South Bohemia in České Budějovice

Faculty of Science

Nucleoside inhibitors of tick-borne encephalitis virus

RNDr. Thesis

Mgr. Luděk Eyer, Ph.D.

České Budějovice
2015

Eyer, L. 2015: **Nucleoside inhibitors of tick-borne encephalitis virus.** RNDr. Thesis, in English 11 p., Faculty of Science, University of South Bohemia, České Budějovice, Czech Republic.

Annotation:

In this work, a series of nucleoside analogues was tested for the ability to inhibit the replication of tick-borne encephalitis virus (TBEV) in porcine kidney cells and human neuroblastoma cells. The interactions of three nucleoside analogues with viral polymerase were simulated using advanced computational methods. The nucleoside analogues 7-deaza-2'-C-methyladenosine (7-deaza-2'-CMA), 2'-C-methyladenosine (2'-CMA), and 2'-C-methylcytidine (2'-CMC) inhibited TBEV replication. These compounds showed dose-dependent inhibition of TBEV-induced cytopathic effects, TBEV replication and viral antigen production. Notably, 2'-CMC was relatively cytotoxic to porcine kidney cells. The anti-TBEV effect of 2'-CMA in cell culture diminished gradually after day 3 posttreatment. 7-Deaza-2'-CMA showed no detectable cellular toxicity, and the antiviral effect in culture was stable for > 6 days posttreatment. High antiviral activity and low cytotoxicity suggest that 7-deaza-2'-CMA is a promising candidate for further investigation as a potential therapeutic agent in treating TBEV infection.

Declaration (in Czech):

Prohlašuji, že svoji rigorózní práci jsem vypracoval samostatně pouze s použitím pramenů a literatury uvedených v seznamu citované literatury.

Prohlašuji, že v souladu s § 47b zákona č. 111/1998 Sb. v platném znění souhlasím se zveřejněním své rigorózní práce, a to v nezkrácené úpravě elektronickou cestou ve veřejně přístupné části databáze STAG provozované Jihočeskou univerzitou v Českých Budějovicích na jejích internetových stránkách, a to se zachováním mého autorského práva k odevzdanému textu této kvalifikační práce. Souhlasím dále s tím, aby toutéž elektronickou cestou byly v souladu s uvedeným ustanovením zákona č. 111/1998 Sb. zveřejněny posudky školitele a oponentů práce i záznam o průběhu a výsledku obhajoby kvalifikační práce. Rovněž souhlasím s porovnáním textu mé kvalifikační práce s databází kvalifikačních prací Theses.cz provozovanou Národním registrem vysokoškolských kvalifikačních prací a systémem na odhalování plagiátů.

V Českých Budějovicích dne .....

Mgr. Luděk Eyer, Ph.D.

This thesis is based on following publication:

Eyer *et al*.: Nucleoside inhibitors of tick-borne encephalitis virus. ANTIMICROBIAL AGENTS AND CHEMOTHERAPY Volume: 59 Issue: 9 Pages: 5483-5493 Published: SEP 2015

Declaration of author's contribution to the study:

Hereby I declare that I had a significant contribution to the following paper. I performed majority of experiments, particularly antiviral in vitro assays, cytotoxicity assays, immnofluorescence staining and dose-response studies with selected antiviral compunds. I participated significantly in the experiment design, data analysis and manuscript preparation.

Agreement of the co-authors

James J. Valdés
Victor A. Gil
Radim Nencka
Hubert Hřebabecký
Michal Šála
Jiří Salát
Jiří Černý
Martin Palus
Erik De Clercq
Daniel Růžek

Acknowledgements

I would like to express my very great appreciation to all co-autors for their assistance, valuable and constructive suggestions during the planning and development of this research work. Especially, I would like to express my deep gratitude to Associate Professor Daniel Růžek, Ph.D. for his patient guidance, enthusiastic encouragement and useful critiques.

Financial support:

This study was supported by Czech Science Foundation projects P502/11/2116 and GA14-29256S and by project LO1218 from the Ministry of Education, Youth and Sports of the Czech Republic under the NPU I program and from AdmireVet project No. CZ 1.05/2.1.00/01.0006-ED 0006/01/01. We acknowledge a grant for the development of research organization (RVO: 61388963), project CZ.1.07/2.3.00/30.0032, which is co-financed by the European Social Fund and the state budget of the Czech Republic, and project PELE (ERC-2009-Adg 25027).

AAC Journals.ASM.org

Nucleoside Inhibitors of Tick-Borne Encephalitis Virus

Luděk Eyer,[a] James J. Valdés,[b] Victor A. Gil,[c] Radim Nencka,[d] Hubert Hřebabecký,[d] Michal Šála,[d] Jiří Salát,[a] Jiří Černý,[a,b,e] Martin Palus,[a,b,e] Erik De Clercq,[f] Daniel Růžek[a,b,e]

Department of Virology, Veterinary Research Institute, Brno, Czech Republic[a]; Institute of Parasitology, Biology Centre of the Czech Academy of Sciences, České Budějovice, Czech Republic[b]; Joint BSC-CRG-IRB Research Program in Computational Biology, Barcelona Supercomputing Center, Barcelona, Spain[c]; Institute of Organic Chemistry and Biochemistry, The Czech Academy of Sciences, Prague, Czech Republic[d]; Faculty of Science, University of South Bohemia, České Budějovice, Czech Republic[e]; Rega Institute for Medical Research, Leuven, Belgium[f]

Tick-borne encephalitis virus (TBEV) is a leading cause of human neuroinfections in Europe and Northeast Asia. There are no antiviral therapies for treating TBEV infection. A series of nucleoside analogues was tested for the ability to inhibit the replication of TBEV in porcine kidney cells and human neuroblastoma cells. The interactions of three nucleoside analogues with viral polymerase were simulated using advanced computational methods. The nucleoside analogues 7-deaza-2′-*C*-methyladenosine (7-deaza-2′-CMA), 2′-*C*-methyladenosine (2′-CMA), and 2′-C-methylcytidine (2′-CMC) inhibited TBEV replication. These compounds showed dose-dependent inhibition of TBEV-induced cytopathic effects, TBEV replication (50% effective concentrations [EC_{50}]of 5.1 ± 0.4 μM for 7-deaza-2′-CMA, 7.1 ± 1.2 μM for 2′-CMA, and 14.2 ± 1.9 μM for 2′-CMC) and viral antigen production. Notably, 2′-CMC was relatively cytotoxic to porcine kidney cells (50% cytotoxic concentration [CC_{50}] of ~50 μM). The anti-TBEV effect of 2′-CMA in cell culture diminished gradually after day 3 posttreatment. 7-Deaza-2′-CMA showed no detectable cellular toxicity (CC_{50} > 50 μM), and the antiviral effect in culture was stable for >6 days posttreatment. Computational molecular analyses revealed that compared to the other two compounds, 7-deaza-2′-CMA formed a large cluster near the active site of the TBEV polymerase. High antiviral activity and low cytotoxicity suggest that 7-deaza-2′-CMA is a promising candidate for further investigation as a potential therapeutic agent in treating TBEV infection.

Tick-borne encephalitis virus (TBEV) belongs to the *Flaviviridae* family, which includes other human- and animal-pathogenic viruses of global importance, such as West Nile virus (WNV), dengue virus (DENV), Japanese encephalitis virus (JEV), yellow fever virus (YFV), and hepatitis C virus (HCV) (1). TBEV virions are approximately 50 nm in diameter and are composed of a spherical nucleocapsid surrounded by a host-derived lipid bilayer. The TBEV genome is a single-stranded, plus-sense RNA about 11 kb in length that encodes a single polyprotein; this polyprotein is co- and posttranslationally processed into 3 structural and 7 nonstructural proteins (2).

In Europe and Northeast Asia, tick-borne encephalitis (TBE) represents one of the most important and serious neuroviral infections. More than 13,000 clinical cases of TBE, including numerous deaths, are reported annually worldwide (3, 4). The considerable increase in TBE incidence in countries where it is endemic and the emergence of the disease in several Western and Northern European countries have made TBE an increasing public health risk. In Europe, the most affected areas are southern Germany, Switzerland, Austria, the Czech Republic, Slovakia, Hungary, Slovenia, the Baltic states, Poland, parts of Scandinavia, and European Russia (5). The disease is usually biphasic: the first stage is febrile with flu-like symptoms, while the second phase manifests most often as meningitis, encephalitis, meningoencephalitis, meningoencephalomyelitis, and radiculitis. There are long-lasting or permanent neuropsychiatric sequelae in 10 to 20% of the infected patients (6). Although human vaccines against TBEV are currently available, the vaccination coverage remains quite low in several of the countries where TBEV is endemic (7). No specific antiviral therapy has been developed for TBE, and patient treatment is limited to supportive care (8). There is thus an urgent need for an effective approach to treatment that is based on specific inhibitors of TBEV replication.

Chemically modified nucleosides, also called nucleoside analogues or nucleoside inhibitors, represent the largest class of antiviral drugs. These compounds generally act via DNA or RNA chain termination with the potential exception of ribavirin, for which the mechanism may depend upon the virus and experimental system (9). Nucleoside analogues have been widely used as inhibitors of numerous medically important viruses, including HIV, herpesvirus, and hepatitis B virus (10, 11). Regarding flaviviruses, nucleoside analogues have been demonstrated to be efficacious in HCV replicon assays (12–16) and also against DENV (17–21), WNV (22), and YFV (23). Some of them were described as broad-spectrum inhibitors of various RNA viruses (24–27). 2′-Modified nucleoside analogues exhibit a high antiflavivirus activity and good pharmacokinetic properties (9). For TBEV inhibition, however, these compounds have not been tested thoroughly, if they have been tested at all. The high degree of homology between the polymerases of TBEV and other flaviviruses (28) suggests, however, that an investigation of nucleoside analogues as inhibitors of TBEV would be worthwhile.

Received 4 April 2015 **Returned for modification** 28 April 2015
Accepted 18 June 2015

Accepted manuscript posted online 29 June 2015

Citation Eyer L, Valdés JJ, Gil VA, Nencka R, Hřebabecký H, Šála M, Salát J, Černý J, Palus M, De Clercq E, Růžek D. 2015. Nucleoside inhibitors of tick-borne encephalitis virus. Antimicrob Agents Chemother 59:5483–5493. doi:10.1128/AAC.00807-15.

Address correspondence to Daniel Růžek, ruzekd@paru.cas.cz.

Supplemental material for this article may be found at http://dx.doi.org/10.1128/AAC.00807-15.

Copyright © 2015, American Society for Microbiology. All Rights Reserved.

doi:10.1128/AAC.00807-15

Downloaded from http://aac.asm.org/ on August 15, 2015 by guest

In the present study, a series of nucleoside analogues were tested for the ability to inhibit TBEV replication in cell culture. Particular attention was paid to chemically modified nucleosides that have reported antiviral activity against other flaviviruses, especially HCV (14) or hemorrhagic fever-associated flaviviruses (i.e., Alkhurma hemorrhagic fever virus, Omsk hemorrhagic fever virus, and Kyasanur Forest disease virus) (29). Compounds with favorable inhibitory profiles in the virus titer reduction assays were further assayed for the ability to inhibit virus-induced cytopathic effects and to suppress viral antigen expression in infected cell cultures. The lead compounds were subsequently evaluated for dose-response inhibition of TBEV replication and for potential cytotoxic effects on host cells. Based on these screens, we identified three compounds with strong anti-TBEV activity. The favorable characteristics of one of these compounds, 7-deaza-2′-*C*-methyladenosine (7-deaza-2′-CMA), indicate that it merits further investigation as a therapeutic agent for treating TBEV infections.

MATERIALS AND METHODS

Cell cultures, virus strains, and antiviral compounds. Porcine kidney stable (PS) cells were cultured at 37°C in Leibovitz (L-15) medium supplemented with 3% precolostral calf serum and a 1% mixture of penicillin and glutamine (Sigma-Aldrich, Prague, Czech Republic) (30). Human neuroblastoma UKF-NB-4 cells were cultured at 37°C in 5% CO_2 in Iscove's modified Dulbecco's medium (IMDM) supplemented with 10% fetal bovine serum and a 1% mixture of penicillin and streptomycin (Sigma-Aldrich) (31). All experiments were performed with TBEV strains Hypr and Neudoerfl, which are representatives of the West European TBEV subtype. Ribavirin and 2′-*C*-methyladenosine (2′-CMA) were synthesized at the Institute of Organic Chemistry and Biochemistry (Prague, Czech Republic). 7-deaza-2′-*C*-methyladenosine (7-deaza-2′-CMA), 2′-*C*-methylcytidine (2′-CMC), and 6-azauridine were purchased from Carbosynth (Compton, United Kingdom). Mericitabine was purchased from ChemScene (Monmouth Junction, NJ). The test compounds were solubilized in 100% (vol/vol) dimethyl sulfoxide (DMSO) to yield 10 mM stock solutions.

Viral titer reduction assay. PS or UKF-NB-4 cells were seeded in 96-well plates (approximately 2×10^4 cells per well) and incubated for 24 h to form a confluent monolayer. Following incubation, the medium was aspirated from the wells and replaced with 200 μl of fresh medium containing a 50 μM concentration of the test compound (three wells per compound). The cells were immediately infected with the Hypr or Neudoerfl TBEV strain at a multiplicity of infection (MOI) of 0.1. As a negative control, DMSO was added to virus- and mock-infected cells at a final concentration of 0.5% (vol/vol). After 72 h of incubation, the medium was collected and immediately frozen at −80°C. Viral titers were determined by plaque assay.

Plaque assay. Virus titers were assayed using PS cell monolayers as described previously (32). Briefly, 10-fold dilutions of TBEV were prepared in 24-well tissue culture plates, and PS cells were added in suspension (0.6×10^5 to 1.5×10^5 cells per well). After a 4-h incubation, the suspension was overlaid with 1.5% (wt/vol) carboxymethylcellulose in L-15 medium. Following a 5-day incubation at 37°C, the infected plates were washed with phosphate-buffered saline (PBS) and the cell monolayers were stained with naphthalene black. The virus titer was expressed as PFU per milliliter.

CPE inhibition assay and CPE quantification. The PS cells were seeded in 96-well plates, the test compounds were added, and the cells were infected with TBEV as described for the viral titer reduction assay. Culture medium was collected 3 to 4 days postinfection (p.i.) to yield a 40 to 50% cytopathic effect (CPE) in virus control wells. The CPE was monitored visually using an Olympus BX-5 microscope equipped with an Olympus DP-70 charge-coupled-device (CCD) camera. To quantify the CPE, both cell death and viability were determined using commercially available colorimetric *in vitro* assays. Cell death was evaluated using the CytoTox 96 nonradioactive cytotoxicity assay (Promega, WI) by following the manufacturer's instructions. This assay is based on quantitative measurement of lactate dehydrogenase, a stable cytosolic enzyme that is released upon cell lysis. Cell death was estimated as the percentage of colorimetric absorbance at 490 nm by the compound-treated cells relative to the absorbance by chemically lysed cells. Cell viability was evaluated by determining formazan exclusion in confluent cell cultures in a colorimetric assay utilizing Dojindo's highly water-soluble tetrazolium salt (Cell Counting Kit-8; Dojindo Molecular Technologies, MD). Cell viability was expressed as the percentage of absorbance at 450 nm by compound-treated cells relative to the absorbance by DMSO-treated cells.

Immunofluorescence staining. PS cells were cultured on slides treated with the test compound (0 to 50 μM) and infected with the TBEV Hypr strain at an MOI of 0.1. At day 4 postinfection, the cells were subjected to cold acetone-methanol (1:1) fixation for 10 min, rinsed in saline, and blocked with 10% fetal bovine serum. Cells were labeled with a mouse monoclonal antibody that recognizes the flavivirus group surface antigen (1:250; Sigma-Aldrich, Prague, Czech Republic) by incubation for 1 h at 37°C. After a washing with saline-Tween 20 (0.05% [vol/vol]), the cells were labeled with an anti-mouse goat secondary antibody conjugated with fluorescein isothiocyanate (FITC) (1:500) by incubation for 1 h at 37°C. The cells were counterstained with 4′,6-diamidino-2-phenylindole (DAPI) (1 μg ml^{-1}; Sigma-Aldrich) for 30 min at 37°C and mounted in 2.5% 1,4-diazabicyclo[2.2.2]octane (DABCO; Sigma-Aldrich). The images were acquired with an Olympus IX71 epifluorescence microscope equipped with a Hammamatsu OrcaR2 camera and controlled using Xcellence software. The images were processed using Fiji software (33).

Cytotoxicity assays. PS cell monolayers in 96-well plates were treated with test compounds at a concentration range of 0 to 50 μM (2-fold dilutions, three wells per concentration). At 4 days p.i., the potential cytotoxicity of test compounds was determined in terms of cell viability and death using Cell Counting Kit-8 (Dojindo Molecular Technologies) and the CytoTox 96 nonradioactive cytotoxicity assay (Promega, WI), respectively, as described for CPE quantification. The concentration of compound that reduced cell viability by 50% was considered the 50% cytotoxic concentration (CC_{50}).

Dose-response studies with 2′-CMA, 7-deaza-2′-CMA, and 2′-CMC. PS cell monolayers that were cultured for 24 h in 96-well plates were treated with 200 μl of medium containing the test compounds (2′-CMA, 7-deaza-2′-CMA, and 2′-CMC) at concentrations from 0 to 50 μM (2-fold dilution, three wells per concentration) and infected with the TBEV Hypr strain at an MOI of 0.1. The medium was collected from the wells at 1-day intervals (postinfection days 1 to 6), and the viral titers were determined by plaque assays. The obtained virus titers were utilized to construct TBEV growth curves and dose-response curves for selected nucleoside inhibitors. The dose-response curves on postinfection days 3 and 4 were used to estimate the most widely used measures of drug potency: the 50% effective concentration (EC_{50}; the concentration of compound required to inhibit the viral titer by 50% compared to the control value), the selectivity index ($SI = CC_{50}/EC_{50}$), and the slope value (Hill coefficient). The EC_{50}s were calculated as follows: a dose-response inhibition curve was fitted to a four parameter logistic curve using Prism 5.04 software (GraphPad, Inc., CA) according to the equation $Y = \text{Bottom} + (\text{Top} - \text{Bottom})/[1 + 10^{\text{Hill coefficient}(\log EC_{50} - X)}]$. In this equation, X is the logarithm of the concentration, Y is the logarithm of the titer, bottom and top correspond to the asymptotes of the sigmoidal curve, Hill coefficient corresponds to the slope at the inflection point of the curve, and log EC_{50} is the calculated midpoint of the curve. The EC_{50} was calculated as $10^{\log EC_{50}}$. The standard errors of the EC_{50}s were estimated by the delta method.

Computer-aided protein modeling and preparation, and protein-ligand exploration and clustering. The crystal structures of viral polymerases from HCV (PDB codes 1nb4 and 1nb6), WNV (PDB code 2hfz),

Downloaded from http://aac.asm.org/ on August 15, 2015 by guest

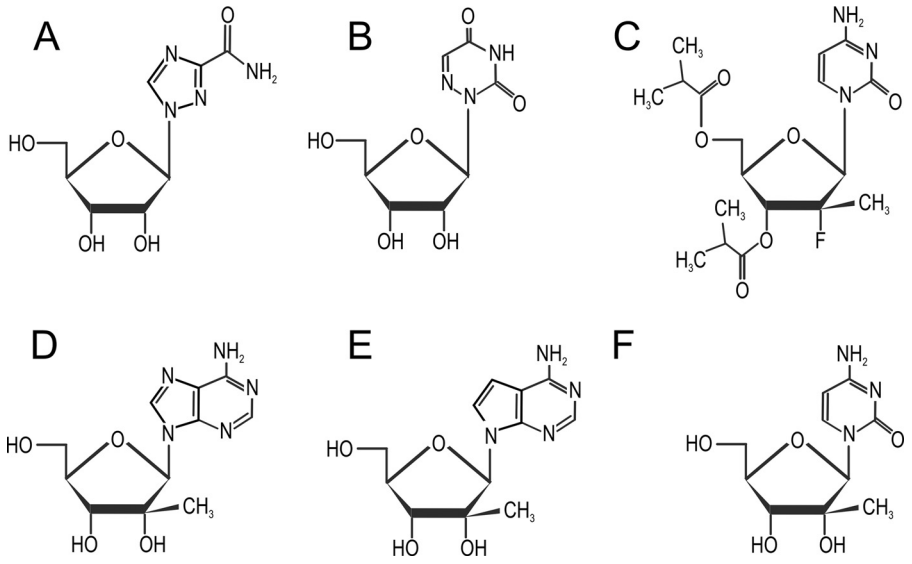

FIG 1 The structures of the nucleoside analogues tested in this study. (A) Ribavirin; (B) 6-azauridine; (C) mericitabine; (D) 2′-CMA; (E) 7-deaza-2′-CMA; (F) 2′-CMC.

and JEV (PDB code 4k6m) were used for computer simulations that would complement the experimental results from this study. The TBEV structure was modeled using Modeler (34). The models were evaluated using the protein model-qualifying servers ModFOLD, QMEAN, and RESPROX (35–37). Based on a consensus, the best-ranked TBEV model was then selected for subsequent *in silico* experiments. Since X-ray crystallography methods do not resolve hydrogen atoms, Schrödinger's Maestro Protein Preparation Wizard was used for each viral polymerase structure to assign hydrogen atoms and to optimize the assigned hydrogen-bond network (38). The respective ligands for each protein structure were removed prior to preparation. After protein preparation, an energy minimization (using the default conditions in Schrödinger's Maestro package) (39) was performed for each crystal structure, including the modeled TBEV polymerase structure, to alter the initial conformation and to remove any steric clashes prior to simulations. In addition, the HCV-UTP bound structure (PDB code 1nb6) has two Mn^{2+} ions as cofactors, with several water molecules surrounding the nucleoside. These were also added to all structures and remained constrained for all subsequent simulations.

We used the Protein Energy Landscape Explorer (PELE) algorithm to perform protein-ligand simulations of the three nucleoside triphosphate analogues identified in this study and the aforementioned viral polymerases. For the simulations, we used the triphosphate form of the nucleoside analogues (2′-CMA-TP, 2′-CMC-TP, and 7-deaza-2′-CMA-TP) since they are phosphorylated *in vivo*. A detailed explanation of the PELE algorithm can be found in references (40 and 41), and its many uses can be seen at https://pele.bsc.es/. Briefly, PELE performs three steps. First, localized ligand perturbations and protein perturbations are performed using an anisotropic network model (ANM) (42) to move the alpha-carbon backbone toward a new position after minimization. Second, PELE optimizes amino acid side chains in proximity of the ligand using steric filters and a rotamer library (43). Finally, PELE uses a truncated Newton minimizer and a surface generalized implicit solvent for minimization, achieving a local minimum after the initial perturbation (44). These steps are repeated for a desired number of iterations and are performed in parallel using several computer-processing units (CPUs). The output is a series of trajectories that represent conformational changes of the side chains and ligand exploration. A Monte Carlo Metropolis criterion is implemented in the PELE algorithm that accepts or rejects these trajectories based on their calculated energies: if they are equal to or less than (accepts) or greater than (rejects) the initial calculated energy (45). To calculate the energy, the PELE algorithm uses a standard force field that describes the potential energy of a molecular system, known as optimized potentials for liquid simulations (OPLS-2005) (46). The only parameters that were altered from the unconstrained ligand migration ready-made script provided by the PELE server were the ANM type, which was set to 4, and the addition of ANM mode 6 for favorable protein perturbations. The number of iterations was increased to 2,000 for increased sampling.

Cluster analysis was performed for the TBEV PELE simulations using pyProCT (47), a Python cluster analysis tool specifically adapted for biomolecules. Regular cluster analysis methods require a deep understanding of the data set and the algorithm. In addition, these methods are sensitive to small changes in its parameters. Instead of forcing users to perform a blind analysis, pyProCT implements a hypothesis-driven protocol. First, the user employs domain knowledge to characterize the desired result in terms of measurable clustering attributes (e.g., maximum and minimum number of clusters, size, noise, cluster separation, etc.) Second, the software searches the clustering space to obtain the clusters that best fit the hypothesis. The same script was used for each nucleoside triphosphate analogue in the PELE protein-ligand exploration simulations of the TBEV-modeled polymerase. The script instructs pyProCT to calculate the distances of each nucleoside using (i) an iterative superposition of the protein backbone and (ii) the calculated distances between the heavy atoms and the geometrical center of the ligand. The K-medoids, DBSCAN, spectral clustering, hierarchical (single-linkage), and GROMOS clustering algorithms were used, with up to 50 parameterizations for each one. The allowed clusterings had to have 3 to 20 clusters with a minimum of 300 elements. No more than 20% of the elements could be tagged as noise. The evaluation function that chose the best clustering was a combination of the silhouette index and a naive cohesion measure. This choice of evaluation functions favors results in which the clusters are well separated with a special emphasis on their compactness. Finally, the "atomic_distances" postprocessing option was used in order to obtain a human-readable file with the per-element distances between serine 331 (Ser331) of the TBEV modeled polymerase and the ligand as well as the per-cluster statistics.

RESULTS

Inhibition of TBEV growth, TBEV-induced CPE, and viral antigen expression. Six nucleoside analogues with chemical modifi-

Downloaded from http://aac.asm.org/ on August 15, 2015 by guest

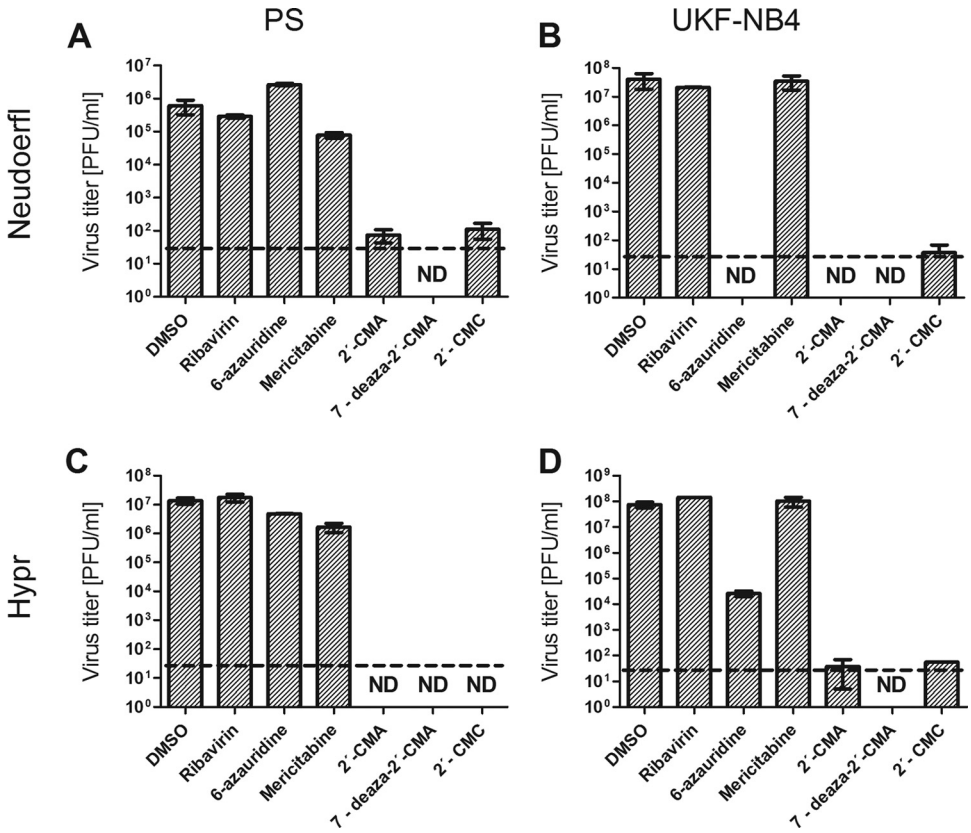

FIG 2 Reduction of TBEV titers by the indicated nucleoside analogues. PS or UKF-NB-4 cells were infected with TBEV (Hypr or Neudoerfl strain) at a multiplicity of infection of 0.1 and treated with nucleoside analogues at 50 μM. The TBEV titers were determined by the plaque assay 3 days postinfection. DMSO-treated cells were used as a negative control. Bars show the mean values from three biological replicate wells, and the error bars indicate the standard errors of the means ($n = 3$). ND, not detected (below the detection limit). Horizontal dashed lines indicate the minimum detectable threshold of 1.44 $\log_{10}$ PFU ml^{-1}.

cations of the ribose or purine/pyrimidine moiety (Fig. 1) were tested for the ability to inhibit the growth of the Hypr and Neudoerfl TBEV strains *in vitro* in PS cells and human neuroblastoma cells. The compounds were tested at a concentration of 50 μM, and the inhibition of TBEV growth was investigated in the culture supernatants 3 days p.i. using a plaque assay.

The Hypr and Neudoerfl TBEV strains (MOI of 0.1) reached mean peak titers of 10^7 and 10^6 PFU/ml, respectively, in PS cells at 3 days p.i. In human neuroblastoma cells, both TBEV strains reached a viral titer of approximately 10^8 PFU/ml at 3 days p.i. Three of the nucleoside analogues tested, 7-deaza-2′-CMA, 2′-CMA, and 2′-CMC, inhibited the growth of both TBEV strains in PS cells and in human neuroblastoma cells. In PS cells, treatment with 50 μM each compound reduced virus titers 10^4- to 10^7-fold compared to that in a mock-treated culture (Fig. 2A and B). Even greater viral titer reduction (10^6- to 10^8-fold) was observed in TBEV-infected human neuroblastoma cells (Fig. 2C and D).

Ribavirin and mericitabine showed weak or no anti-TBEV effects in PS cells and human neuroblastoma cells. 6-Azauridine showed no antiviral effect in PS cells; however, this compound significantly reduced the viral titer (10^3-fold for Hypr and 10^6-fold for Neudoerfl) in human neuroblastoma cells (Fig. 2B and D).

To verify the primary screening results, we next investigated the compounds using the CPE inhibition assay. Inhibition of TBEV-induced CPE in PS cells in the presence of the test compounds was monitored using light microscopy 3 to 4 days p.i. The TBEV Hypr strain had a strong CPE on the target PS cells on day 3 p.i. in the absence of nucleoside inhibitors (Fig. 3A). A strong CPE was also observed in PS cell cultures treated with ribavirin (Fig. 3A), mericitabine, and 6-azauridine (see Fig. S1B and C in the supplemental material), indicating that these compounds had no protective effects on the survival and growth of PS cells exposed to TBEV. 6-Azauridine was highly cytotoxic, causing cell death and morphological changes in PS cells. Both adenosine derivatives, i.e., 7-deaza-2′-CMA and 2′-CMA, completely inhibited the CPE at concentrations of 50 μM and had no adverse morphological effects on growing cells. However, a relatively strong CPE was observed in 2′-CMC-treated PS cell monolayers (Fig. 3A).

The CPE of 7-deaza-2′-CMA, 2′-CMA, and 2′-CMC on TBEV-infected PS cells was evaluated quantitatively in terms of cell viability and death using two independent colorimetric *in vitro* assays. Mock-treated TBEV-infected PS cells showed a high rate of cell death, i.e., 46% dead cells, at day 4 p.i. (Fig. 3B; see Fig. S2 in the supplemental material). TBEV-infected PS cells treated with either 7-deaza-2′-CMA or 2′-CMA showed a low rate of cell death (11 to 15%) and high viability (95 to 105%). The measured values were close to the cell death and viability values determined for mock-treated uninfected PS cells (11% and 100%, respectively) that were used as negative controls (Fig. 3B; see also Fig. S2 in the supplemental material). The results strongly indicate that

Downloaded from http://aac.asm.org/ on August 15, 2015 by guest

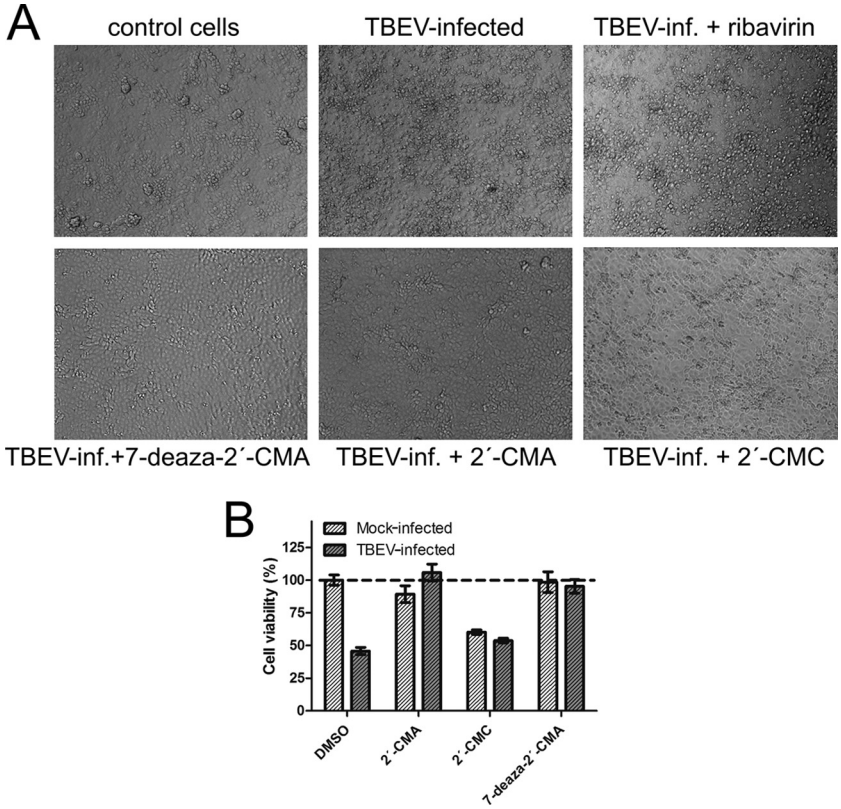

FIG 3 Inhibition of the TBEV-induced cytopathic effect by the indicated nucleoside analogues. PS cells were infected with TBEV strain Hypr at a multiplicity of infection of 0.1 and were left untreated (DMSO) or treated with 50 μM ribavirin, 7-deaza-2′-CMA, 2′-CMA, or 2′-CMC. Inhibition of the CPE was monitored on day 3 or 4 postinfection (A). (B) Quantification of the CPE in TBEV-infected and mock-infected cells treated with 50 μM 2′-CMA, 2′-CMC, or 7-deaza-2′-CMC. The CPE was expressed as the percentage of cell viability at day 4 postinfection. The horizontal dashed line indicates cell viability and cell death in DMSO-treated uninfected cells (control). The bars indicate the means, and error bars indicate SEMs ($n = 3$).

7-deaza-2′-CMA and 2′-CMA at concentrations of 50 μM completely protected PS cells from TBEV, allowing them to survive in the presence of TBEV with no apparent cytotoxicity. For 2′-CMC, development of the CPE was marked by increased cell death (26 to 28%) and decreased cell viability (54 to 60%) (Fig. 3B; see also Fig. S2).

The antiviral effect of 7-deaza-2′-CMA, 2′-CMA and 2′-CMC was further confirmed by immunofluorescence staining, which was used to assess the expression of the TBEV surface E antigen in PS cells as an index of viral infectivity and replication *in vitro*. The TBEV surface E antigen was strongly expressed in TBEV-infected mock-treated cells (Fig. 4), and no virus antigen was detected in mock-infected PS cells (data not shown). Immunofluorescence staining revealed that 7-deaza-2′-CMA, 2′-CMA, and 2′-CMC at concentrations of 50 μM completely inhibited the expression of the TBEV surface E antigen in virus-infected PS cells (Fig. 4). These results correlated with the strong suppression of TBEV growth in the 7-deaza-2′-CMA-, 2′-CMA-, and 2′-CMC-treated cell cultures (Fig. 2A and C).

Cytotoxicities of TBEV inhibitors. The cytotoxicities of 7-deaza-2′-CMA, 2′-CMA, and 2′-CMC were evaluated in PS cells using a cell viability assay (Fig. 5) and subsequently confirmed by a cell death assay (see Fig. S3 in the supplemental material). No cellular toxicity was seen in cultures of PS cells treated with 7-deaza-2′-CMA at concentrations ranging from 0 to 50 μM (CC_{50} >50 μM) 4 days posttreatment (Fig. 5C and Table 1; see also Fig. S3C). A cell viability assay showed similar results with 2′-CMA (CC_{50} > 50 μM). However, 50 μM 2′-CMA moderately increased cell death, by ~22%, at 4 days after drug administration (Fig. 5A and Table 1; see also Fig. S3A) compared to the rate for mock-treated cells (~15%). For both adenosine derivatives, the concentration of 50 μM had no detectable effect on cell proliferation. 2′-CMC showed a dose-dependent cytotoxic effect on PS cell cultures 4 days posttreatment. Based on a cell viability assay, the CC_{50} of 2′-CMC was determined to be ~50 μM (Fig. 5B and Table 1; see also Fig. S3B).

Dose-response antiviral activities of the TBEV inhibitors. The compounds that showed TBEV inhibitory effects in the initial experiments, i.e., 7-deaza-2′-CMA, 2′-CMA, and 2′-CMC, were further evaluated to determine their dose-dependent antiviral activities. PS cells were infected with the Hypr strain (MOI of 0.1) and immediately treated with each compound at a concentration range of 0 to 50 μM. The culture supernatants were then subjected to the plaque assay. TBEV titers in the culture supernatants were assayed daily on days 1 to 6 p.i. The dose-response curves on postinfection days 3 and 4 were used to estimate the EC_{50}, SI, and slope value.

All three compounds reduced the viral titer in a dose-dependent manner (Fig. 6; see also Fig. S4 in the supplemental material). The shape of the dose-response curves for 7-deaza-2′-CMA changed over time from a flat curve on day 1 p.i. to typical sigmoidal curves with relatively steep slopes on days 2 to 6 p.i. (Fig. 6A).

Downloaded from http://aac.asm.org/ on August 15, 2015 by guest

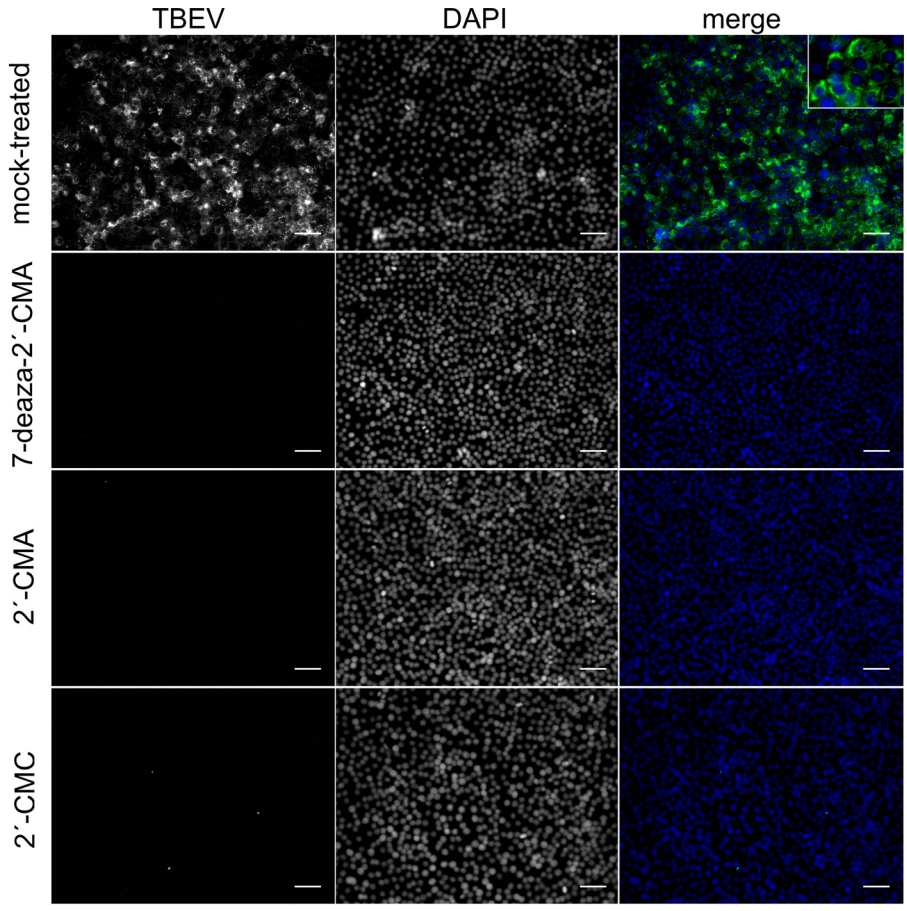

FIG 4 Inhibition of TBEV viral antigen expression by the indicated nucleoside inhibitors. PS cells were infected with TBEV and treated with 0.5% DMSO or with 50 μM 7-deaza-2′-CMA, 2′-CMA, or 2′-CMC. PS cells were fixed on slides at day 4 postinfection and stained with flavivirus-specific antibody labeled with FITC (green) and then counterstained with DAPI (blue). Scale bars, 50 μm.

7-Deaza-2′-CMA reduced the viral titer, showing an EC_{50} of 5.1 ± 0.4 μM and a selectivity index (SI) of >9.8 (Table 1). 7-Deaza-2′-CMA was ineffective in terms of reducing the viral titer at concentrations of 0.1 and 0.5 μM, and the TBEV growth curves were indistinguishable from the TBEV growth curve for mock-treated cells (see Fig. S4A). At a concentration of 3.1 μM, the TBEV inhibitory effect of 7-deaza-2′-CMA became more evident, resulting in ~10^2-fold reduction in the titer relative to that in mock-treated cells. Marked inhibitory effects on TBEV replication were observed at concentrations of 7-deaza-2′-CMA at or above 6.2 μM. When the compound was added at concentrations of 12.5, 25, and 50 μM, there was a significant and steady reduction in viral titer (a 10^6- to 10^7-fold reduction). At these concentrations, 7-deaza-2′-CMA reduced the mean TBEV titers to below the limit of detection (1.44 $\log_{10}$ PFU ml^{-1}) between p.i. days 4 and 6.

A cytidine derivative, 2′-CMC, also showed marked dose-dependent inhibition of TBEV titers. The shape and particularly the slope of the 2′-CMC dose-response curve were similar to those of 7-deaza-2′-CMA (Fig. 6B). However, 2′-CMC was approximately 3-fold less potent in terms of inhibiting TBEV than was 7-deaza-2′-CMA (EC_{50} of 14.2 ± 1.9 μM) (Table 1). The relatively low SI value of ~3.5 was due to the considerable cytotoxicity of the compound for PS cells, as described above. At 0.1, 0.5, and 3.1 μM, 2′-CMC inhibited virus replication weakly or not at all. The inhibitory effects of 2′-CMC became more evident at concentrations of 6.2 to 12.5 μM, with virus titer reduction of about 10^2 at 6 days p.i. 2′-CMC completely suppressed TBEV replication at concentrations of 25 and 50 μM; there was a 10^4- to 10^6-fold reduction in viral titer during the experimental period (see Fig. S4B in the supplemental material).

2′-CMA showed a significant dose-dependent antiviral effect only at day 3 p.i. (Fig. 6C). The 2′-CMA dose-response curve was characterized by an EC_{50} of 7.1 ± 1.2 μM (SI of about 7) and by a relatively low Hill coefficient (0.7 for 2′-CMA versus 2.7 for 7-deaza-2′-CMA and 2.2 for 2′-CMC [Table 1]). At day 3 p.i., 2′-CMA strongly reduced TBEV titers at concentrations of 20 and 50 μM, resulting in >10^5-fold viral titer inhibition relative to that in mock-treated TBEV-infected cells. Although the initial decrease in viral titers was very strong, the inhibitory effects of 2′-CMA diminished gradually after day 3 p.i., regardless of concentration. The decrease in the antiviral effect of 2′-CMA over time allowed the virus titers in 50 μM 2′-CMA-treated cells to rebound to 1.7 × 10^6 PFU/ml at day 6 p.i. (see Fig. S4C).

Exploration of NS5B with nucleoside analogues using PELE. Selection and characterization of drug-resistant HCV replicons revealed that serine 282 (Ser282) determines the efficacy of the inhibitory nucleoside 2′-CMA (13). Figure S5 in the supplemental material illustrates the proof of principle for our PELE-based ex-

Downloaded from http://aac.asm.org/ on August 15, 2015 by guest

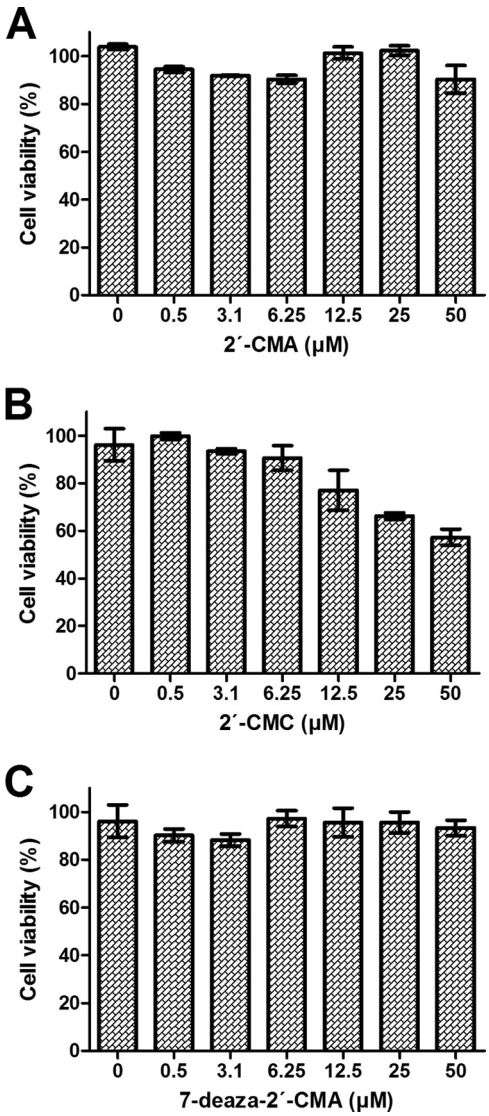

FIG 5 Cytotoxicity of the indicated nucleoside inhibitors. Cytotoxicity was determined by incubating PS cells with the indicated concentrations of 2′-CMA (A), 2′-CMC (B), or 7-deaza-2′-CMA (C) and is expressed in terms of cell viability and cell death at day 4 postinfection. The bars indicate the mean values from three replicate wells, and the error bars indicate the SEMs.

ploration of nucleoside triphosphate analogues with viral polymerases. In the bound crystal structure of HCV (PDB code 1nb6), the distance between the alpha carbon of Ser282 and the geometric center of the heavy atoms of UTP is 9.3 Å as measured using the Maestro package (39). Figure S5 shows that for the most part, UTP explores ~20 to 70 Å away from the Ser282 in both the bound and unbound (or apoenzyme) crystal structures of the HCV polymerase. In both cases, however, there was UTP exploration <20 Å away from the Ser282 (encircled in Fig. S5), and this separate cluster approaches the native position of the bound HCV-UTP complex (*y* axes in Fig. S5; i.e., the geometric center position of all heavy atoms of UTP in PDB code 1nb6).

To further validate the results of the nucleoside triphosphate analogue exploration, we simulated the experimental results reported by Migliaccio et al. (13), who investigated the inhibitory effect of 2′-CMA using HCV and other phylogenetically related viruses *in vitro*. Figure S6A in the supplemental material shows the exploration of 2′-CMA-triphosphate (2′-CMA-TP) in proximity to the homologous serine residue of the viral polymerases of the HCV (PDB code 1nb6), WNV (PDB code 2hfz), and JEV (PDB code 4k6m) crystal structures. This analysis showed that 2′-CMA-TP spent the majority of the exploration away from the homologous serine residue. Further investigation of whether 2′-CMA is an effective inhibitor of JEV is needed since no such experiments have been reported. Figure S6B shows that the three effective nucleoside triphosphate analogues used in the current study, i.e., 2′-CMA-TP, 2′-CMC-TP, and 7-deaza-2′-CMA-TP, also explored in proximity to the Ser331 of the modeled tertiary structure of TBEV NS5B (the residue homologous to HCV Ser282).

The results from the clustering analysis are summarized in Table S1 in the supplemental material. Visual inspection of all three nucleoside triphosphate analogue clusters for the TBEV polymerase showed two types of clusters. The first type was generated by a partition of the space sampled in the exploration of each nucleoside. Since this zone was densely populated, it was difficult to find a good balance between cluster compactness and separation (which would penalize the silhouette index). The second type of cluster had better-defined boundaries since these clusters formed "natural" aggregates that were created as the nucleoside explored the protein surface in proximity to Ser331 of the TBEV polymerase. From this second group or second type of cluster, we selected those that were <18 Å from the alpha carbon of Ser331 (green areas in Fig. 7A). The logic behind this cutoff criterion is depicted graphically in Fig. S5 in the supplemental material, i.e., the encircled cluster. During the exploration of the HCV polymerase, UTP approaches the binding site (*y* axes in Fig. S5; 2 to 12 Å from its native position) as it "cuts off" from the majority of the modeling for exploration (18 to 20 Å from Ser282; *x* axes in Fig. S5).

All three simulations showed a large cluster (colored the same shade of green in Fig. 7B) with more than half of its elements in proximity to Ser 331 (especially for 7-deaza-2′-CMA-TP). For 2′-CMA-TP and 2′-CMC-TP, there were elements of other clusters (colored different shades of green in Fig. 7B) that also seemed to be in proximity to Ser331 of the TBEV polymerase. Assuming that phylogenetically related viral polymerases have similar binding sites, we used the central position of UTP bound to HCV (PDB code 1nb6) to geometrically determine the pathway toward the predicted binding site of TBEV. The scatter plots in Fig. 7C show that the majority of modeling for the exploration is away from Ser331 (i.e., the first type of cluster; >20 Å). Each scatter plot, however, has a linear correlation (r^2) of >0.9, approaching the predicted binding site of the TBEV polymerase, which is clearly shown by the large single cluster of 7-deaza-2′-CMA-TP (Fig. 7).

TABLE 1 Characteristics of selected TBEV-inhibiting nucleosides

Compound	EC_{50}, μM[a]	Hill coefficient[a]	CC_{50}, μM[a] (viability assay)	SI (CC_{50}/EC_{50})
7-deaza-2′-CMA	5.1 ± 0.4	2.7 ± 0.5	>50	>9.8
2′-CMA	7.1 ± 1.2	0.7 ± 0.1	>50	>7.0
2′-CMC	14.2 ± 1.9	2.2 ± 0.5	~50	~3.5

[a] Determined from three independent experiments.

Downloaded from http://aac.asm.org/ on August 15, 2015 by guest

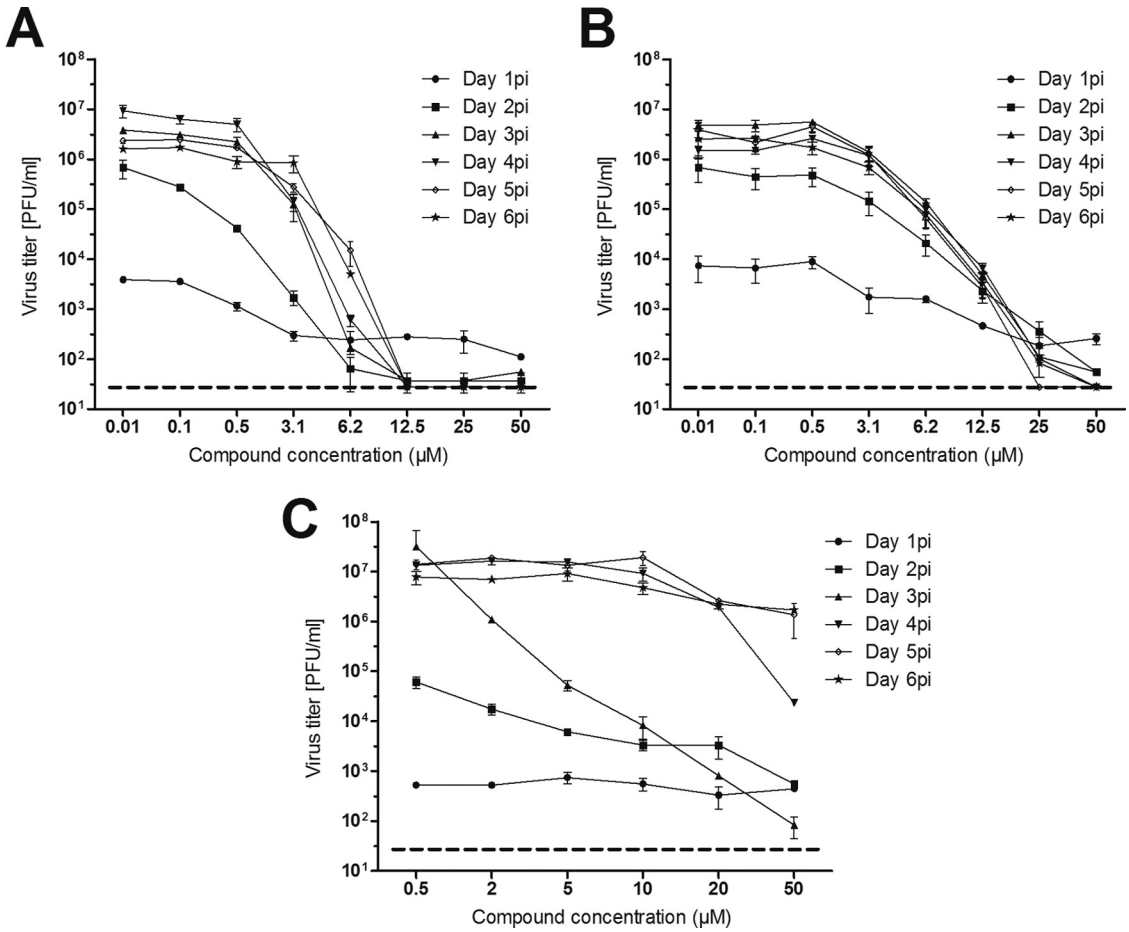

FIG 6 Dose-dependent effect of the indicated TBEV inhibitors on virus titers. PS cells were infected with TBEV at a multiplicity of infection of 0.1 and treated with 7-deaza-2′-CMA (A), 2′-CMC (B), or 2′-CMA (C) at the indicated concentrations. TBEV titers were monitored at days 1 to 6 postinfection. The mean titers from three biological replicates are shown, and error bars indicate SEMs ($n = 3$). The horizontal dashed line indicates the minimum detectable threshold of 1.44 $\log_{10}$ PFU ml^{-1}.

DISCUSSION

TBE is a substantial public health problem in some parts of Europe and Asia. At present, there is no specific treatment for TBE other than supportive care. Few studies have tested potential TBEV inhibitors (48), and there is an urgent need for safe, efficient drugs for treating patients with TBE. In this study, a series of nucleoside analogues that were previously reported to inhibit members of the *Flaviviridae* family were tested for the ability to suppress TBEV replication. We could not determine the structure-activity relationship for all of the compounds in this study, although this will be the subject of a future investigation.

The anti-TBEV activity of the compounds was determined in PS cells and in human neuroblastoma cells. PS cells are widely used for TBEV isolation and for multiplication and plaque assays (30). Human neuroblastoma cells are highly sensitive to TBEV infection and represent a valuable model for neuropathogenesis studies of TBEV as well as for studies of several other neurotropic viruses (31). The initial screening was performed using two TBEV strains, Neudoerfl and Hypr, which represent two virulence models. Neudoerfl, the European prototype TBEV strain, exhibits medium virulence, while the Hypr strain is highly virulent (49). Although ribavirin, 6-azauridine, and mericitabine have been described as potent inhibitors of several flaviviruses (29, 41, 50), these compounds did not reproducibly inhibit TBEV *in vitro* at concentrations of 50 μM. 6-Azauridine has been reported in the literature to be relatively well tolerated by several host cell lines as well as being well tolerated *in vivo* (29). However, in our experiments, this compound had a strong cytotoxic effect on both PS cells (see Fig. S1C in the supplemental material) and human neuroblastoma cells (data not shown), resulting in significantly reduced viral titers in 6-azauridine-treated human neuroblasts (Fig. 2B and D).

Three 2′-*C*-methyl-substituted nucleosides, 2′-CMC, 2′-CMA, and 7-deaza-2′-CMA, strongly inhibited the *in vitro* growth of TBEV in both cell lines and were selected as lead candidate compounds for further testing. 2′-CMC was recently tested for its ability to inhibit replication of yellow fever virus (23), Alkhurma hemorrhagic fever virus, Kyasanur Forest disease virus, and Omsk hemorrhagic fever virus (29). Moreover, the 3′-valyl ester of 2′-CMC, valopicitabine, showed viral load reductions in patients infected with genotype 1 HCV in clinical trials, although it was subsequently discontinued for the treatment of hepatitis C (55, 56). Our results indicate that 2′-CMC had strong antiviral activity against both the Hypr and Neudoerfl TBEV strains; however, this

Downloaded from http://aac.asm.org/ on August 15, 2015 by guest

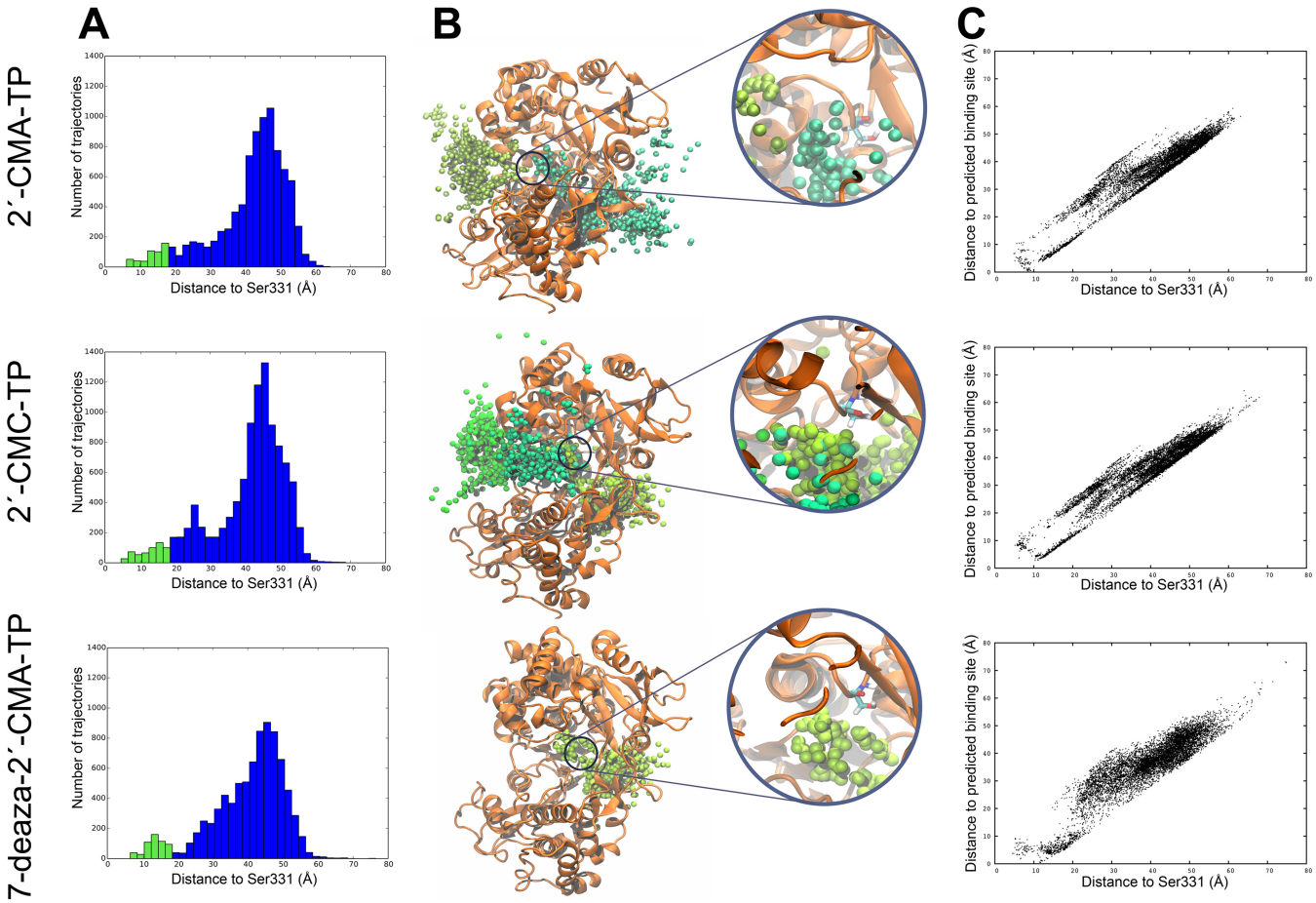

FIG 7 Cluster analyses of nucleoside triphosphate analogue exploration of the TBEV polymerase. (A) The distance for each of the studied nucleoside triphosphate analogues (2′-CMA-TP, 2′-CMC-TP, and 7-deaza-2′-CMA-TP) are shown in the histograms. The 0- to 18-Å range, which denotes the proximity toward Ser331 (*x* axes), is colored light green. (B) Tertiary representations of the selected clusters for each system. Each nucleoside is represented by its C-7 atom. (C) Scatter plots depict the approach of each nucleoside toward the predicted binding site of TBEV.

compound was cytotoxic for PS cells (CC_{50} of about 50 μM). The substitution of cytosine for adenine in 2′-CMA, a compound that has recently been used for experimental therapy of HCV and DENV infections (18, 51), significantly reduced the cytotoxicity for both cell lines and increased the anti-TBEV inhibitory effect of the compound. However, viral replication gradually rebounded after 3 days in the treated cultures (Fig. 6C). The observed decrease in antiviral activity of 2′-CMA and the rebound in viral titer were probably related to the rapid deamination of 2′-CMA by cellular adenosine deaminase to the inactive inosine derivative (52). Such an intracellular deamination is described as an undesirable effect in the inhibitory activity of 2′-CMA against HCV replication, resulting in poor bioavailability and rapid clearance of 2′-CMA in plasma (14). 2′-CMA could be also inactivated by cellular phosphorylases, which are enzymes that catalyze phosphorolysis of the purine glycosidic bond (12). Alternatively, the evolution of 2′-CMA-resistant TBEV mutants could explain the observed viral titer rebound (53).

The incorporation of the 7-deaza moiety into the 2′-CMA molecule eliminated cytotoxicity in both PS cells and human neuroblastoma cells. The potency of 7-deaza-2′-CMA to inhibit TBEV replication was comparable to that of 2′-CMA and was approximately 3-fold higher than that of 2′-CMC. The inhibitory effect of 7-deaza-2′-CMA was stable over the 6-day experimental period, and there was no rebound in viral titer during this period. The 7-deaza-purine substitution is described as an important modification of the nucleobase that strongly affects the biological properties of the nucleoside analogue. The 7-deaza modification alters the glycosyl torsion angle, which may change the glycosyl bond length. This could lead to a rearrangement in the general electronic character of the purine base and, in particular, to disruption of the alignment of the 3′-hydroxyl function for nucleophilic attack on the alpha phosphorus of the next incoming NTP. The 7-deaza modification may, therefore, result in enhanced potency of the nucleoside analogue in terms of terminating viral RNA synthesis (9, 14). Due to the antiviral activity and low cytotoxicity of 7-deaza-2′-CMA, this nucleoside derivative has been widely tested to determine whether it inhibits the RNA replication of other medically important flaviviruses. For example, 7-deaza-2′-CMA inhibits HCV replication with an EC_{50} of 0.3 μM with no apparent cytotoxicity and shows promising pharmacokinetic properties in several animal species, including primates (14, 54). Similar antiviral properties have been demonstrated for the 7-deaza-substituted derivative of 2′-C-acetylene-adeno-

Downloaded from http://aac.asm.org/ on August 15, 2015 by guest

sine, which was recently reported to suppress DENV replication in the transient-replicon assay and in a mouse model (18).

To understand the efficacies of 2′-CMA, 2′-CMC, and 7-deaza-2′-CMA for inhibiting TBEV, we simulated the exploration of the TBEV polymerase by the triphosphate form of each nucleoside analogue (Fig. 7). The computational simulations showed that these inhibitors sampled toward the binding site of the TBEV polymerase. There are a couple of other clusters that aggregate toward the TBEV binding site for 2′-CMA-TP and 2′-CMC-TP. Based on our experimental results, we infer that the pathway is represented by the single cluster of 7-deaza-2′-CMA-TP in Fig. 7, but a more robust analysis must be performed to confirm this hypothesis. Takhampunya et al. (41) developed a method for calculating the ligand/drug binding free energy during its exploration toward the active site of a protein. Their results showed strong correlations with experimental data. We are currently using such methods to determine the viral polymerase binding pathways of 2′-CMA, 2′-CMC, and 7-deaza-2′-CMA and their binding free energies.

In conclusion, we identified three compounds with activity against TBEV *in vitro*. These compounds will be tested further in a mouse model of TBEV infection. These compounds, even if they are not clinically effective, may be useful research tools or starting points for drug development efforts against TBEV. Because of its high antiviral activity and low cytotoxicity, 7-deaza-2′-CMA is an attractive candidate for further investigation as a potential therapeutic agent not only for TBE treatment but also for treating other flaviviral neuroinfections.

ACKNOWLEDGMENTS

We are greatly indebted to Jan Kopecký and Libor Grubhoffer for general support of our work, to Ivana Huvarová for excellent technical assistance, to Vladimír Babák for statistical data processing, and to Jiří Volf for preparation of the immunofluorescence images.

This study was supported by Czech Science Foundation projects P502/11/2116 and GA14-29256S and by project LO1218 from the Ministry of Education, Youth and Sports of the Czech Republic under the NPU I program and by AdmireVet project no. CZ 1.05/2.1.00/01.0006-ED 0006/01/01. We acknowledge a grant for the development of research organization (RVO: 61388963). J.J.V. was supported by project CZ.1.07/2.3.00/30.0032, which is cofinanced by the European Social Fund and the state budget of the Czech Republic. V.A.G. was sponsored by the European project PELE (ERC-2009-Adg 25027).

The funders played no role in study design, data collection and analysis, the decision to publish, or the preparation of the manuscript.

REFERENCES

1. **Baier A.** 2011. Flaviviral infections and potential targets for antiviral therapy, p 89–104. *In* Ruzek D (ed), Flavivirus encephalitis. InTech, Rijeka, Croatia.
2. **Chambers TJ, Hahn CS, Galler R, Rice CM.** 1990. Flavivirus genome organization, expression, and replication. Annu Rev Microbiol **44:**649–688. http://dx.doi.org/10.1146/annurev.mi.44.100190.003245.
3. **Dumpis U, Crook D, Oksi J.** 1999. Tick-borne encephalitis. Clin Infect Dis **28:**882–890. http://dx.doi.org/10.1086/515195.
4. **Heinz FX, Mandl CW.** 1993. The molecular biology of tick-borne encephalitis virus. APMIS **101:**735–745. http://dx.doi.org/10.1111/j.1699-0463.1993.tb00174.x.
5. **Heinz FX, Stiasny K, Holzmann H, Grgic-Vitek M, Kriz B, Essl A, Kundi M.** 2013. Vaccination and tick-borne encephalitis, Central Europe. Emerg Infect Dis **19:**69–76. http://dx.doi.org/10.3201/eid1901.120458.
6. **Ruzek D, Dobler G, Mantke OD.** 2010. Tick-borne encephalitis: pathogenesis and clinical implications. Travel Med Infect Dis **8:**223–232. http://dx.doi.org/10.1016/j.tmaid.2010.06.004.
7. **Zavadska D, Anca I, Andre F, Bakir M, Chlibek R, Cizman M, Ivaskeviciene I, Mangarov A, Meszner Z, Pokorn M, Prymula R, Richter D, Salman N, Simurka P, Tamm E, Tesovic G, Urbancikova I, Usonis V.** 2013. Recommendations for tick-borne encephalitis vaccination from the Central European Vaccination Awareness Group (CEVAG). Hum Vaccin Immunother **9:**362–374. http://dx.doi.org/10.4161/hv.22766.
8. **Puig-Basagoiti F, Tilgner M, Forshey BM, Philpott SM, Espina NG, Wentworth DE, Goebel SJ, Masters PS, Falgout B, Ren P, Ferguson DM, Shi PY.** 2006. Triaryl pyrazoline compound inhibits flavivirus RNA replication. Antimicrob Agents Chemother **50:**1320–1329. http://dx.doi.org/10.1128/AAC.50.4.1320-1329.2006.
9. **De Clercq E, Neyts J.** 2009. Antiviral agents acting as DNA or RNA chain terminators. Handb Exp Pharmacol **189:**53–84. http://dx.doi.org/10.1007/978-3-540-79086-0_3.
10. **De Clercq E.** 2004. Antivirals and antiviral strategies. Nat Rev Microbiol **2:**704–720. http://dx.doi.org/10.1038/nrmicro975.
11. **De Clercq E.** 2011. A 40-year journey in search of selective antiviral chemotherapy. Annu Rev Pharmacol Toxicol **51:**1–24. http://dx.doi.org/10.1146/annurev-pharmtox-010510-100228.
12. **Eldrup AB, Allerson CR, Bennett CF, Bera S, Bhat B, Bhat N, Bosserman MR, Brooks J, Burlein C, Carroll SS, Cook PD, Getty KL, MacCoss M, McMasters DR, Olsen DB, Prakash TP, Prhavc M, Song QL, Tomassini JE, Xia J.** 2004. Structure-activity relationship of purine ribonucleosides for inhibition of hepatitis C virus RNA-dependent RNA polymerase. J Med Chem **47:**2283–2295. http://dx.doi.org/10.1021/jm030424e.
13. **Migliaccio G, Tomassini JE, Carroll SS, Tomei L, Altamura S, Bhat B, Bartholomew L, Bosserman MR, Ceccacci A, Colwell LF, Cortese R, De Francesco R, Eldrup AB, Getty KL, Hou XS, LaFemina RL, Ludmerer SW, MacCoss M, McMasters DR, Stahlhut MW, Olsen DB, Hazuda DJ, Flores OA.** 2003. Characterization of resistance to non-obligate chain-terminating ribonucleoside analogs that inhibit hepatitis C virus replication in vitro. J Biol Chem **278:**49164–49170. http://dx.doi.org/10.1074/jbc.M305041200.
14. **Olsen DB, Eldrup AB, Bartholomew L, Bhat B, Bosserman MR, Ceccacci A, Colwell LF, Fay JF, Flores OA, Getty KL, Grobler JA, LaFemina RL, Markel EJ, Migliaccio G, Prhavc M, Stahlhut MW, Tomassini JE, MacCoss M, Hazuda DJ, Carroll SS.** 2004. A 7-deaza-adenosine analog is a potent and selective inhibitor of hepatitis C virus replication with excellent pharmacokinetic properties. Antimicrob Agents Chemother **48:**3944–3953. http://dx.doi.org/10.1128/AAC.48.10.3944-3953.2004.
15. **Klumpp K, Leveque V, Le Pogam S, Ma H, Jiang WR, Kang HS, Granycome C, Singer M, Laxton C, Hang JQ, Sarma K, Smith DB, Heindl D, Hobbs CJ, Merrett JH, Symons J, Cammack N, Martin JA, Devos R, Najera I.** 2006. The novel nucleoside analog R1479 (4′-azidocytidine) is a potent inhibitor of NS5B-dependent RNA synthesis and hepatitis C virus replication in cell culture. J Biol Chem **281:**3793–3799. http://dx.doi.org/10.1074/jbc.M510195200.
16. **Klumpp K, Kalayanov G, Ma H, Le Pogam S, Leveque V, Jiang WR, Inocencio N, De Witte A, Rajyaguru S, Tai E, Chanda S, Irwin MR, Sund C, Winqist A, Maltseva T, Eriksson S, Usova E, Smith M, Alker A, Najera I, Cammack N, Martin JA, Johansson NG, Smith DB.** 2008. 2′-Deoxy-4′-azido nucleoside analogs are highly potent inhibitors of hepatitis C virus replication despite the lack of 2′-alpha-hydroxyl groups. J Biol Chem **283:**2167–2175. http://dx.doi.org/10.1074/jbc.M708929200.
17. **Yin Z, Chen YL, Schul W, Wang QY, Gu F, Duraiswamy J, Kondreddi RR, Niyomrattanakit P, Lakshminarayana SB, Goh A, Xu HY, Liu W, Liu B, Lim JY, Ng CY, Qing M, Lim CC, Yip A, Wang G, Chan WL; Tan HP, Lin K, Zhang B, Zou G, Bernard KA, Garrett C, Beltz K, Dong M, Weaver M, He H, Pichota A, Dartois V, Keller Thomas H, Shi PY.** 2009. An adenosine nucleoside inhibitor of dengue virus. Proc Natl Acad Sci U S A **106:**20435–20439. http://dx.doi.org/10.1073/pnas.0907010106.
18. **Chen YL, Yin Z, Duraiswamy J, Schul W, Lim CC, Liu B, Xu HY, Qing M, Yip A, Wang G, Chan WL, Tan HP, Lo M, Liung S, Kondreddi RR, Rao R, Gu H, He H, Keller TH, Shi PY.** 2010. Inhibition of dengue virus RNA synthesis by an adenosine nucleoside. Antimicrob Agents Chemother **54:**2932–2939. http://dx.doi.org/10.1128/AAC.00140-10.
19. **Chen YL, Yin Z, Lakshminarayana SB, Qing M, Schul W, Duraiswamy J, Kondreddi RR, Goh A, Xu HY, Yip A, Liu B, Weaver M, Dartois V, Keller TH, Shi PY.** 2010. Inhibition of dengue virus by an ester prodrug of an adenosine analog. Antimicrob Agents Chemother **54:**3255–3261. http://dx.doi.org/10.1128/AAC.00397-10.
20. **Latour DR, Jekle A, Javanbakht H, Henningsen R, Gee P, Lee I, Tran P, Ren S, Kutach AK, Harris SF, Wang SM, Lok SJ, Shaw D, Li J, Heilek**

Downloaded from http://aac.asm.org/ on August 15, 2015 by guest

G, Klumpp K, Swinney DC, Deval J. 2010. Biochemical characterization of the inhibition of the dengue virus RNA polymerase by beta-D-2′-ethynyl-7-deaza-adenosine triphosphate. Antiviral Res **87:**213–222. http://dx.doi.org/10.1016/j.antiviral.2010.05.003.

21. **Lee JC, Tseng CK, Wu YH, Kaushik-Basu N, Lin CK, Chen WC, Wu HN.** 2015. Characterization of the activity of 2′-C-methylcytidine against dengue virus replication. Antiviral Res **116:**1–9. http://dx.doi.org/10.1016/j.antiviral.2015.01.002.
22. **Chen H, Liu L, Jones SA, Banavali N, Kass J, Li Z, Zhang J, Kramer LD, Ghosh AK, Li H.** 2013. Selective inhibition of the West Nile virus methyltransferase by nucleoside analogs. Antiviral Res **97:**232–239. http://dx.doi.org/10.1016/j.antiviral.2012.12.012.
23. **Julander JG, Jha AK, Choi JA, Jung KH, Smee DF, Morrey JD, Chu CK.** 2010. Efficacy of 2′-C-methylcytidine against yellow fever virus in cell culture and in a hamster model. Antiviral Res **86:**261–267. http://dx.doi.org/10.1016/j.antiviral.2010.03.004.
24. **Smee DF, Morris JLB, Barnard DL, Vanaerschot A.** 1992. Selective inhibition of arthropod-borne and arenaviruses in vitro by 3′-fluoro-3′-deoxyadenosine. Antiviral Res **18:**151–162. http://dx.doi.org/10.1016/0166-3542(92)90035-4.
25. **Smee DF, Alaghamandan HA, Ramasamy K, Revankar GR.** 1995. Broad-spectrum activity of 8-chloro-7-deazaguanosine against RNA virus infections in mice and rats. Antiviral Res **26:**203–209. http://dx.doi.org/10.1016/0166-3542(94)00084-L.
26. **Ojwang JO, Ali S, Smee DF, Morrey JD, Shimasaki CD, Sidwell RW.** 2005. Broad-spectrum inhibitor of viruses in the Flaviviridae family. Antiviral Res **68:**49–55. http://dx.doi.org/10.1016/j.antiviral.2005.06.002.
27. **Chatelain G, Debing Y, De Burghgraeve T, Zmurko J, Saudi M, Rozenski J, Neyts J, Van Aerschot A.** 2013. In search of flavivirus inhibitors: evaluation of different tritylated nucleoside analogues. Eur J Med Chem **65:**249–255. http://dx.doi.org/10.1016/j.ejmech.2013.04.034.
28. **Koonin EV, Dolja VV.** 1993. Evolution and taxonomy of positive-strand RNA viruses—implications of comparative analysis of amino acid sequences. Crit Rev Biochem Mol Biol **28:**375–430. http://dx.doi.org/10.3109/10409239309078440.
29. **Flint M, McMullan LK, Dodd KA, Dodd KA, Bird BH, Khristova ML, Nichol ST, Spiropoulou CF.** 2014. Inhibitors of the tick-borne, hemorrhagic fever-associated flaviviruses. Antimicrob Agents Chemother **58:**3206–3216. http://dx.doi.org/10.1128/AAC.02393-14.
30. **Kozuch O, Mayer V.** 1975. Pig kidney epithelial (ps) cells—perfect tool for study of flavi-viruses and some other arboviruses. Acta Virol **19:**498.
31. **Růzek D, Vancova M, Tesarova M, Ahantarig A, Kopecky J, Grubhoffer L.** 2009. Morphological changes in human neural cells following tick-borne encephalitis virus infection. J Gen Virol **90:**1649–1658. http://dx.doi.org/10.1099/vir.0.010058-0.
32. **De Madrid AT, Porterfield JS.** 1969. A simple micro-culture method for study of group B arboviruses. Bull World Health Organ **40:**113–121.
33. **Schindelin J, Arganda-Carreras I, Frise E, Kaynig V, Longair M, Pietzsch T, Preibisch S, Rueden C, Saalfeld S, Schmid B, Tinevez JY, White DJ, Hartenstein V, Eliceiri K, Tomancak P, Cardona A.** 2012. Fiji: an open-source platform for biological-image analysis. Nat Methods **9:**676–682. http://dx.doi.org/10.1038/nmeth.2019.
34. **Sali A, Blundell TL.** 1993. Comparative protein modeling by satisfaction of spatial restraints. J Mol Biol **234:**779–815. http://dx.doi.org/10.1006/jmbi.1993.1626.
35. **McGuffin LJ, Buenavista MT, Roche DB.** 2013. The ModFOLD4 server for the quality assessment of 3D protein models. Nucleic Acids Res **41:**W368–W372. http://dx.doi.org/10.1093/nar/gkt294.
36. **Benkert P, Kuenzli M, Schwede T.** 2009. QMEAN server for protein model quality estimation. Nucleic Acids Res **37:**W510–W514. http://dx.doi.org/10.1093/nar/gkp322.
37. **Berjanskii M, Zhou J, Liang Y, Lin G, Wishart DS.** 2012. Resolution-by-proxy: a simple measure for assessing and comparing the overall quality of NMR protein structures. J Biomol NMR **53:**167–180. http://dx.doi.org/10.1007/s10858-012-9637-2.
38. **Li X, Jacobson MP, Zhu K, Zhao S, Friesner RA.** 2007. Assignment of polar states for protein amino acid residues using an interaction cluster decomposition algorithm and its application to high resolution protein structure modeling. Proteins **66:**824–837.
39. **Schrödinger LLC.** 2010. Maestro version 9.1. Schrödinger LLC, New York, NY.
40. **Madadkar-Sobhani A, Guallar V.** 2013. PELE web server: atomistic study of biomolecular systems at your fingertips. Nucleic Acids Res **41:**W322–W328. http://dx.doi.org/10.1093/nar/gkt454.
41. **Takhampunya R, Ubol S, Houng HS, Cameron CE, Padmanabhan R.** 2006. Inhibition of dengue virus replication by mycophenolic acid and ribavirin. J Gen Virol **87:**1947–1952. http://dx.doi.org/10.1099/vir.0.81655-0.
42. **Atilgan AR, Durell SR, Jernigan RL, Demirel MC, Keskin O, Bahar I.** 2001. Anisotropy of fluctuation dynamics of proteins with an elastic network model. Biophys J **80:**505–515. http://dx.doi.org/10.1016/S0006-3495(01)76033-X.
43. **Jacobson MP, Friesner RA, Xiang ZX, Honig B.** 2002. On the role of the crystal environment in determining protein side-chain conformations. J Mol Biol **320:**597–608. http://dx.doi.org/10.1016/S0022-2836(02)00470-9.
44. **Still WC, Tempczyk A, Hawley RC, Hendrickson T.** 1990. Semianalytical treatment of solvation for molecular mechanics and dynamics. J Am Chem Soc **112:**6127–6129. http://dx.doi.org/10.1021/ja00172a038.
45. **Borrelli KW, Vitalis A, Alcantara R, Guallar V.** 2005. PELE: protein energy landscape exploration. A novel Monte Carlo based technique. J Chem Theory Comput **1:**1304–1311.
46. **Jorgensen WL, Tiradorives J.** 1988. The Opls potential functions for proteins—energy minimizations for crystals of cyclic peptides and crambin. J Am Chem Soc **110:**1657–1666. http://dx.doi.org/10.1021/ja00214a001.
47. **Gil VA, Guallar V.** 2014. pyProCT: automated cluster analysis for structural bioinformatics. J Chem Theory Comput **10:**3236–3243. http://dx.doi.org/10.1021/ct500306s.
48. **Osolodkin DI, Kozlovskaya LI, Dueva EV, Dotsenko VV, Rogova YV, Frolov KA, Krivokolysko SG, Romanova EG, Morozov AS, Karganova GG, Palyulin VA, Pentkovski VM, Zefirov NS.** 2013. Inhibitors of tick-borne flavivirus reproduction from structure-based virtual screening. ACS Med Chem Lett **4:**869–874. http://dx.doi.org/10.1021/ml400226s.
49. **Wallner G, Mandl CW, Ecker M, Holzmann H, Stiasny K, Kunz C, Heinz FX.** 1996. Characterisation and complete genome sequences of high- and low-virulence variants of tick-borne encephalitis virus. J Gen Virol **77:**1035–1042. http://dx.doi.org/10.1099/0022-1317-77-5-1035.
50. **Crance JM, Scaramozzino N, Jouan A, Garin D.** 2003. Interferon, ribavirin, 6-azauridine and glycyrrhizin: antiviral compounds active against pathogenic flaviviruses. Antiviral Res **58:**73–79. http://dx.doi.org/10.1016/S0166-3542(02)00185-7.
51. **Carroll SS, Tomassini JE, Bosserman M, Getty K, Stahlhut MW, Eldrup AB, Bhat B, Hall D, Simcoe AL, LaFemina R, Rutkowski CA, Wolanski B, Yang ZC, Migliaccio G, De Francesco R, Kuo LC, MacCoss M, Olsen DB.** 2003. Inhibition of hepatitis C virus RNA replication by 2′-modified nucleoside analogs. J Biol Chem **278:**11979–11984. http://dx.doi.org/10.1074/jbc.M210914200.
52. **Cristalli G, Costanzi S, Lambertucci C, Lupidi G, Vittori S, Volpini R, Camaioni E.** 2001. Adenosine deaminase: functional implications and different classes of inhibitors. Med Res Rev **21:**105–128. http://dx.doi.org/10.1002/1098-1128(200103)21:2<105::AID-MED1002>3.0.CO;2-U.
53. **Kinney RM, Huang CYH, Rose BC, Kroeker AD, Dreher TW, Iversen PL, Stein DA.** 2005. Inhibition of dengue virus serotypes 1 to 4 in Vero cell cultures with morpholino oligomers. J Virol **79:**5116–5128. http://dx.doi.org/10.1128/JVI.79.8.5116-5128.2005.
54. **Carroll SS, Ludmerer S, Handt L, Koeplinger K, Zhang NR, Graham D, Davies ME, MacCoss M, Hazuda D, Olsen DB.** 2009. Robust antiviral efficacy upon administration of a nucleoside analog to hepatitis C virus-infected chimpanzees. Antimicrob Agents Chemother **53:**926–934. http://dx.doi.org/10.1128/AAC.01032-08.
55. **Carroll SS, Koeplinger K, Vavrek M, Zhang NR, Handt L, MacCoss M, Olsen DB, Reddy KR, Sun ZL, van Poelje PD, Fujitaki JM, Boyer SH, Linemeyer DL, Hecker SJ, Erion MD.** 2011. Antiviral efficacy upon administration of a HepDirect prodrug of 2′-c-methylcytidine to hepatitis C virus-infected chimpanzees. Antimicrob Agents Chemother **55:**3854–3860. http://dx.doi.org/10.1128/AAC.01152-10.
56. **Sofia MJ, Chang W, Furman PA, Mosley RT, Ross BS.** 2012. Nucleoside, nucleotide, and non-nucleoside inhibitors of hepatitis C virus NS5B RNA-dependent RNA polymerase. J Med Chem **55:**2481–2531. http://dx.doi.org/10.1021/jm201384j.

Downloaded from http://aac.asm.org/ on August 15, 2015 by guest

Supplementary Figures and Tables

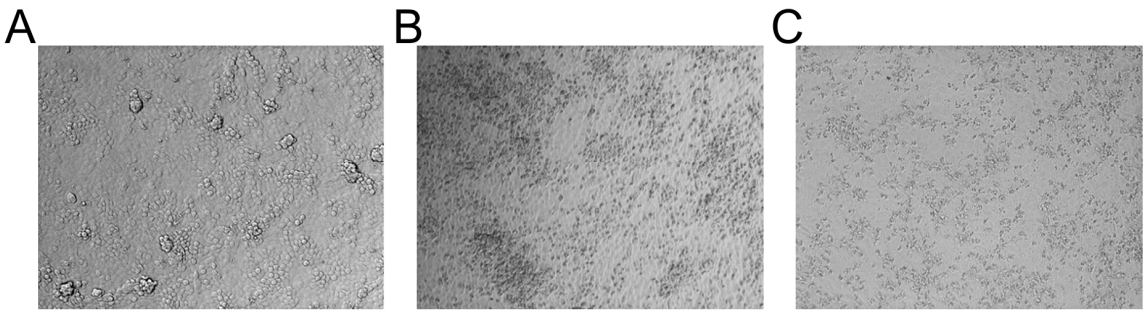

Fig. S1 Untreated PS cells **(A)** or TBEV-infected PS cells treated with 50 µM mericitabine **(B)** or 50 µM 6-azauridine **(C)**. CPE formation was determined at day 3 postinfection.

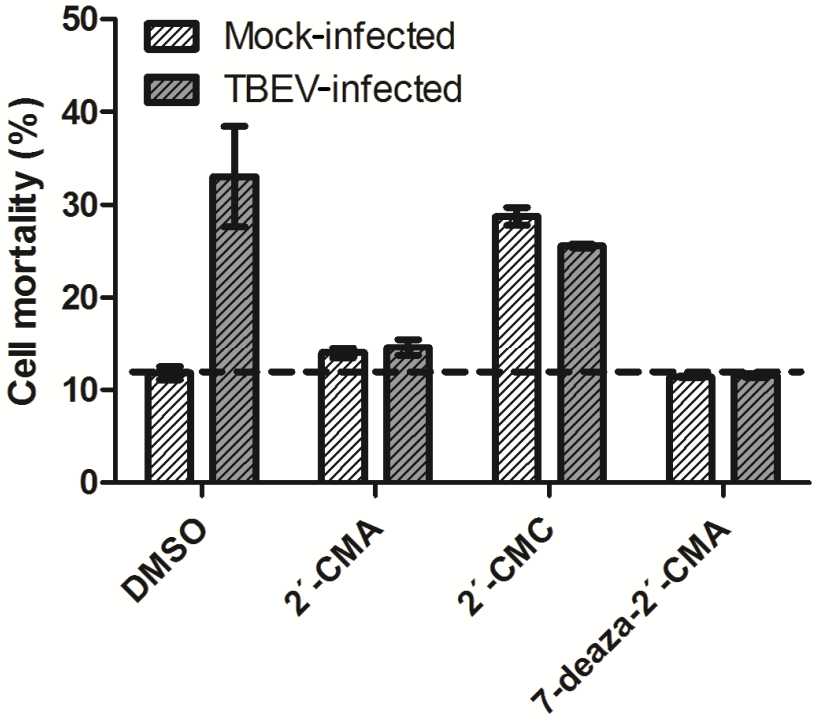

Fig. S2 Inhibition of the TBEV-induced cytopathic effect by the indicated nucleoside analogues. PS cells were infected with TBEV strain Hypr at a multiplicity of infection (MOI) of 0.1 and were left untreated (DMSO) or treated with 50 µM ribavirin, 7-deaza-2´-CMA, 2´-CMA or 2'-CMC. Quantification of the CPE in TBEV-infected and mock-infected cells treated

with 50 μM 2'-CMA, 2'-CMC or 7-deaza-2'-CMC. The CPE was expressed as the percentage of cell death at day 3 postinfection. The horizontal dashed line indicates cell viability and cell death in DMSO-treated non-infected cells (control). The bars indicated the mean ± SEM (n=3).

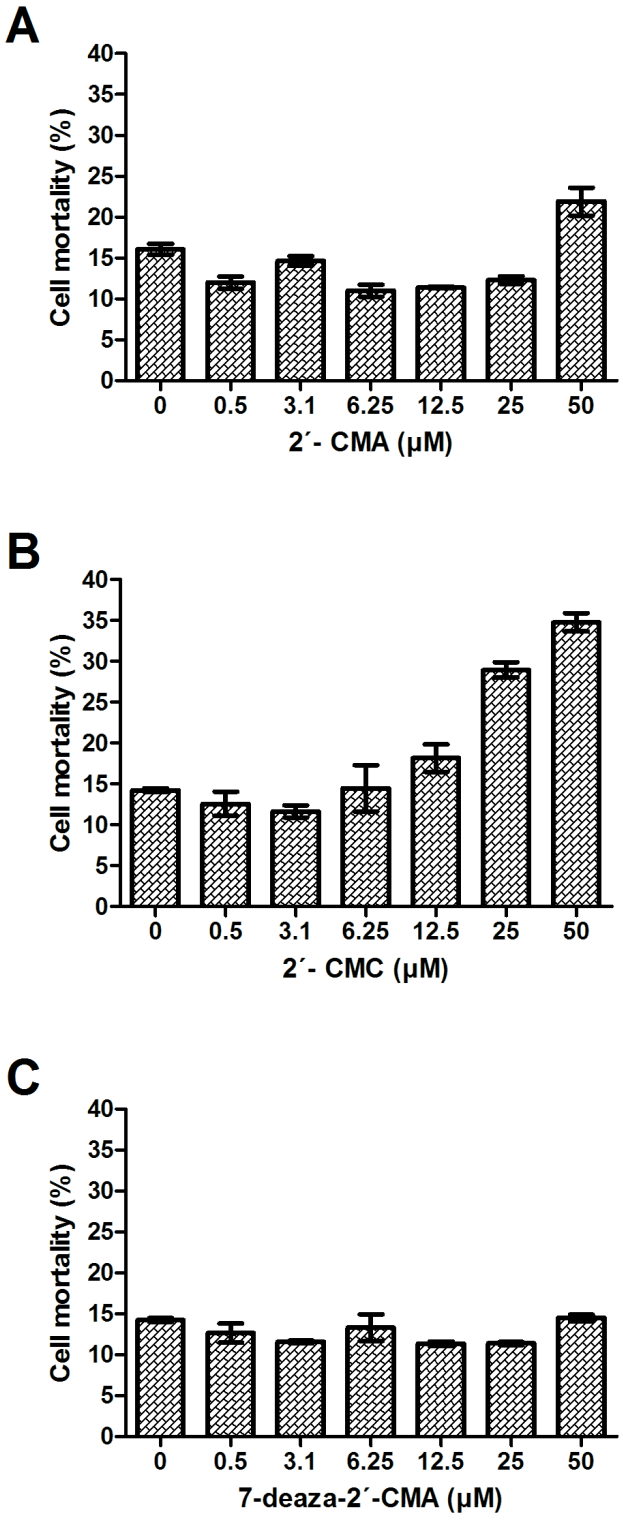

Fig. S3 Cytotoxicity of the indicated nucleoside inhibitors. Cytotoxicity was determined by incubating PS cells with the indicated concentrations of 2'-CMA **(A)**, 2'-CMC **(B)** or 7-deaza-2'-CMA **(C)** and is expressed in terms of cell death at day 3 postinfection. The bars indicated

the mean values from three replicate wells, and the error bars indicate the standard errors of the mean.

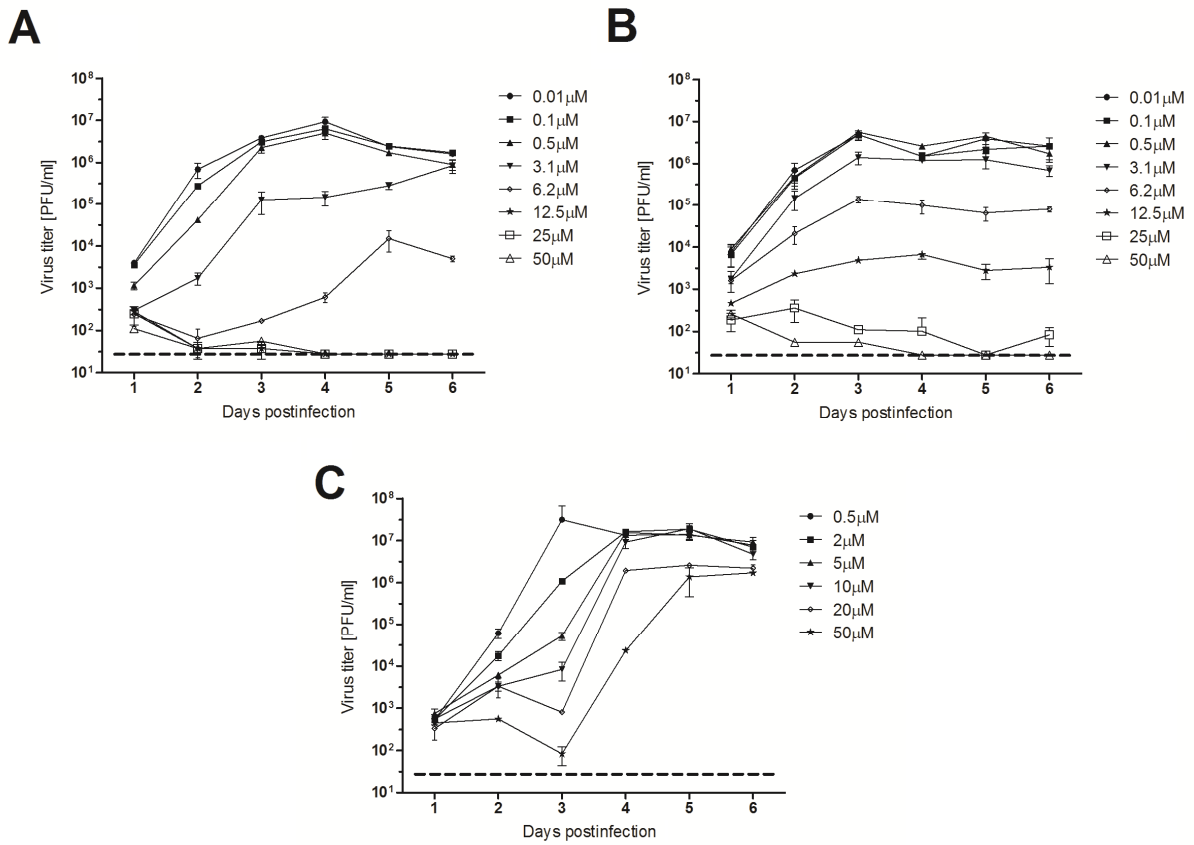

Fig. S4 TBEV Hypr growth curves in PS cells in the presence of the indicated concentrations of the nucleosides. **(A)** 7-deaza-2'-CMC, **(B)** 2'-CMC and **(C)** 2'-CMA. Each data point represents the mean TBEV titre ± SEM determined in triplicate PS culture wells. The horizontal dashed line indicates the minimum detectable threshold of 1.44 $\log_{10}$ PFU mL^{-1}.

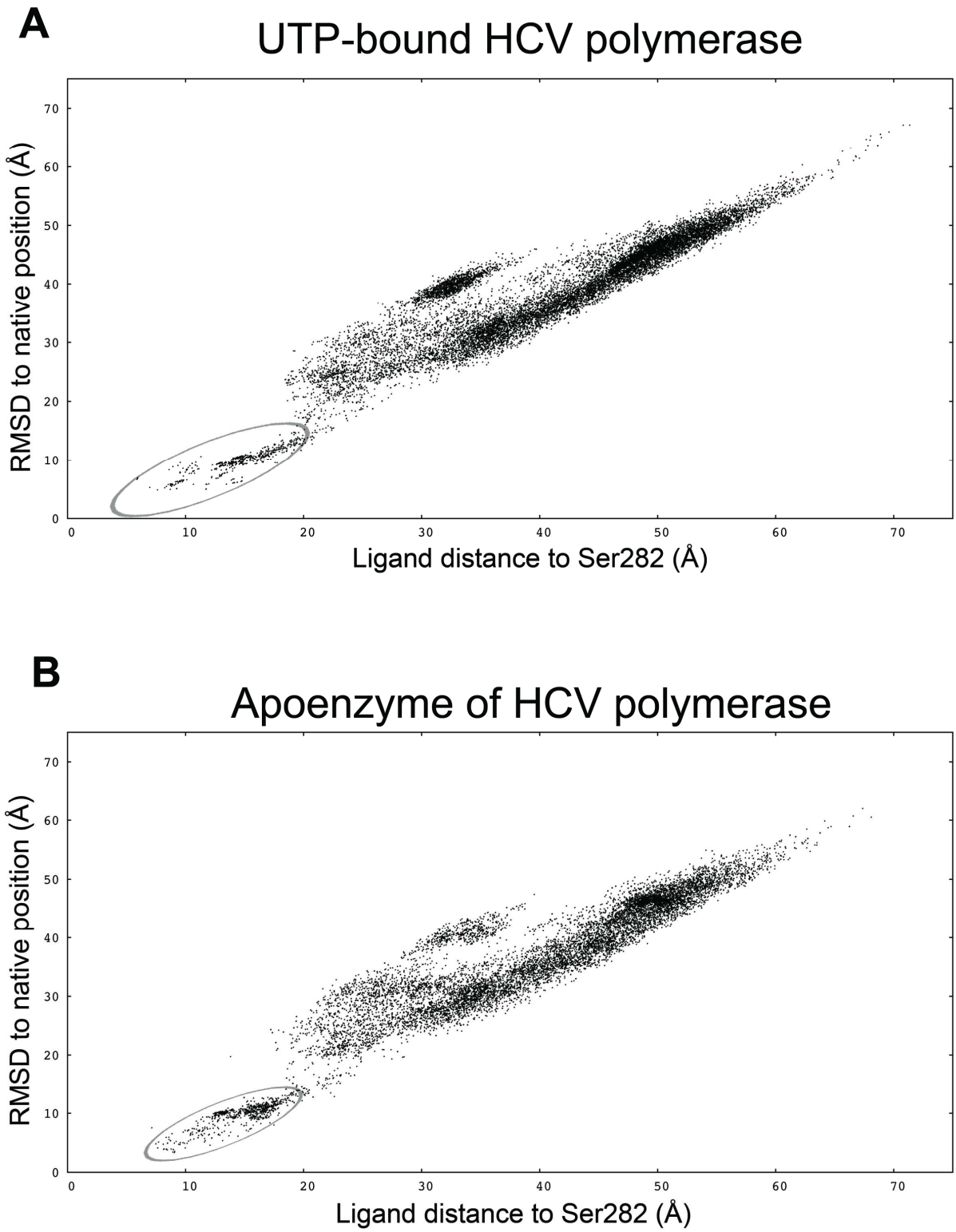

Fig. S5 Computer-aided simulation of structurally characterized nucleoside-viral polymerase interactions. Both panels show that when the nucleoside uridine 5'-triphosphate (UTP) is outside its native position in the original crystal structure of the HCV polymerase (PDB: 1nb6;

similar position for all simulations), the PELE algorithm migrates the ligand near the experimental results, i.e. towards its native position. This was true for both the bound (**A**; PDB: 1nb6) and the unbound/apoenzyme structures (**B**; PDB: 1nb4). The x-axis shows the ligand distance to the Ser282 residue. The y-axis represents the root mean square deviation (RMSD) of each UTP migration trajectory produced by PELE (~15,000 in total) relative to its native position (as in PDB: 1nb6).

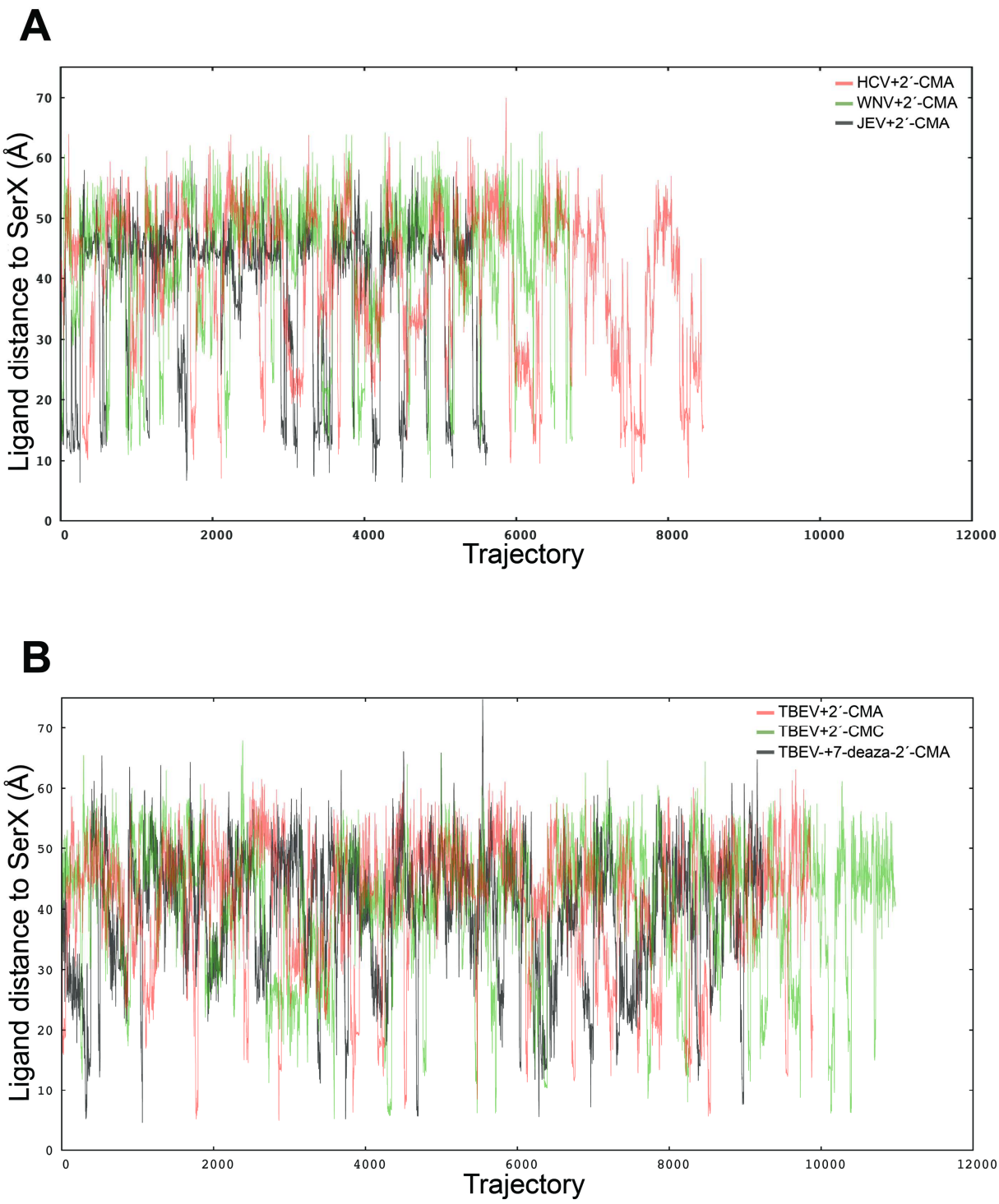

Fig. S6 Nucleoside triphosphate analogue exploration of several phylogenetically-related viral polymerases. The top panel **(A)** shows the PELE simulations using 2'-CMA and the viral polymerase crystal structures of HCV (PDB: 1nb4), WNV (PDB: 2hfz) and JEV (PDB: 4k6m). The bottom panel **(B)** shows the PELE simulations for the TBEV viral polymerase using the nucleoside analogues 2'-CMA, 2'-CMC and 7-deaza-2'-CMA. The y-axes indicate the distance

to the alpha-carbon of the conserved serine residue for each polymerase; the x-axes indicate the trajectories of ligand migration according to PELE.

Table S1. pyProCT output.

Compound	Algorithm[1]	N Clusters[2]	Noise (%)	Silhouette[3]	Cohesion[3]
7-deaza-2´-CMA	k-medoids	12 (16)	9.29	0.42	0.68
2´- CMA	k-medoids	14 (20)	10.6	0.35	0.70
2´-CMC	k-medoids	16 (16)	6.64	0.47	0.74

[1]K-medoids was in all cases the algorithm chosen by pyProCT. This can be explained by the difficulty of partitioning the initial sampling region using other methods.
[2]The N clusters column shows the number of clusters of the result, with the initial k parameter of the k-medoids algorithm in parentheses.
[3]From the silhouette and cohesion indices (ranges of [-1, 1] and [0, 1], respectively), we infer that the resulting clusters are compact but not separated by much.